1993-09

Parametric uncertainty reduction in robust multivariable control

Krueger, David Lawrence.

Monterey, California. Naval Postgraduate School

(2)

NAVAL POSTGRADUATE SCHOOL
Monterey, California

DISSERTATION

PARAMETRIC UNCERTAINTY REDUCTION IN
ROBUST MULTIVARIABLE CONTROL

by

David L. Krueger

September, 1993

Dissertation Supervisors: R. Cristi
J. B. Burl

REPORT DOCUMENTATION PAGE

Form Approved
OMB No. 0704-0188

1. AGENCY USE ONLY (Leave blank)	2. REPORT DATE	3. REPORT TYPE AND DATES COVERED
	September 1993	Doctoral Dissertation

4. TITLE AND SUBTITLE

PARAMETRIC UNCERTAINTY REDUCTION IN ROBUST MULTIVARIABLE CONTROL

5. FUNDING NUMBERS

6. AUTHOR(S)

David L. Krueger

7. PERFORMING ORGANIZATION NAME(S) AND ADDRESS(ES)

Naval Postgraduate School
Monterey, CA 93943-5000

8. PERFORMING ORGANIZATION REPORT NUMBER

9. SPONSORING/MONITORING AGENCY NAME(S) AND ADDRESS(ES)

Director, Strategic Systems Programs
Washington, DC 20376

10. SPONSORING/MONITORING AGENCY REPORT NUMBER

11. SUPPLEMENTARY NOTES

12a. DISTRIBUTION/AVAILABILITY STATEMENT

Approved for public release; distribution is unlimited.

12b. DISTRIBUTION CODE

13. ABSTRACT (Maximum 200 words)

This dissertation presents a method for reducing the number of parametric uncertainties used in the design of a robust H-infinity controller. The resulting controller is shown to meet robust stability and performance requirements in the presence of all the modeled uncertainties. The approach used involves grouping parametric variations affecting the same open loop eigenvalue, then scaling one or more of these variations to accommodate the eigenvalue change caused by all the parametric uncertainties. This method is effective in those cases where a large number of parametric uncertainties cause current computer aided design software to fail to find a robust controller for the plant.

14. SUBJECT TERMS	15. NUMBER OF PAGES	16. PRICE CODE
	105	

17. SECURITY CLASSIFICATION OF REPORT	18. SECURITY CLASSIFICATION OF THIS PAGE	19. SECURITY CLASSIFICATION OF ABSTRACT	20. LIMITATION OF ABSTRACT
UNCLASSIFIED	UNCLASSIFIED	UNCLASSIFIED	UL

NSN 7540-01-280-5500

Standard Form 298 (Rev. 2-89)
Prescribed by ANSI Std. 239.18

Approved for public release; distribution is unlimited.

Parametric Uncertainty Reduction in Robust Multivariable Control
by

David Lawrence Krueger
Lieutenant Commander, United States Navy
B.S., United States Naval Academy, 1979
M.S.A.E., Naval Postgraduate School, 1986

Submitted in partial fulfillment of the
requirements for the degree of

DOCTOR OF PHILOSOPHY IN ELECTRICAL ENGINEERING
from the
NAVAL POSTGRADUATE SCHOOL

September 1993

Author: [redacted]
David L. Krueger

Approved By:

[redacted]
James H. Miller
Associate Professor of
Electrical and Computer Engineering

[redacted]
Harold Titus
Professor of
Electrical and Computer Engineering

[redacted]
Daniel J. Collins
Professor of
Aeronautical and Astronautical Engineering

[redacted]
Anthony Healey
Professor of Mechanical Engineering

[redacted]
Jeffery B. Burl
Assistant Professor of
Electrical Engineering
Michigan Technological University
Dissertation Supervisor

[redacted]
Roberto Cristi
Associate Professor of
Electrical and Computer Engineering
Dissertation Supervisor

Approved by: [redacted]
Michael A. Morgan
Chairman, Department of Electrical and Computer Engineering

Approved by: [redacted]
Richard S. Elster, Dean of Instruction

ABSTRACT

This dissertation presents a method for reducing the number of parametric uncertainties used in the design of a robust H_∞ controller. The resulting controller is shown to meet robust stability and performance requirements in the presence of all the modeled uncertainties. The approach used involves grouping parametric variations affecting the same open loop eigenvalue, then scaling one or more of these variations to accommodate the eigenvalue change caused by all the parametric uncertainties. This method is effective in those cases where a large number of parametric uncertainties cause current computer aided design software to fail to find a robust controller for the plant.

TABLE OF CONTENTS

LIST OF TABLES

LIST OF FIGURES

I. INTRODUCTION

A. PROBLEM STATEMENT

The advent of H_∞ synthesis and associated robust stability analysis techniques has provided a process for designing controllers which are capable of meeting established performance criteria and remaining stable over a wide range of operating conditions and parameter uncertainties. To be successful, however, this process requires that all uncertainties and variations in the plant be quantified and included in the plant model. Modeling the plant in this manner may result in either a high order system or a system severely constrained by the number of uncertainties. Current computer aided design (CAD) software often cannot find a solution when the system order becomes quite large or when a large number of uncertainties are present in the plant model. This does not imply that an appropriate controller does not exist, only that current techniques are inadequate in these cases. A new technique is required that provides for the use of current H_∞ synthesis methods and software, but results in a controller design which is stable and has acceptable performance over all plant variations. In this dissertation we will present a technique for finding a robust H_∞ controller in specific cases where the present design methods fail.

B. HISTORY

The period of modern control is delineated by state-space analysis of systems and the development of optimal Linear Quadratic Gaussian (LQG) controllers. The LQG design techniques, however, largely ignored uncertainties in the system and the stability margins of Linear Quadratic Regulator (LQR) controllers with full state feedback

proved elusive when combined with Kalman Filter estimators (Doyle, 1978). Recently, two new techniques for controller design and stability analysis of multi-input multi-output systems have been introduced, Structured Singular Value analysis and H_∞ synthesis.

Structured Singular Value (SSV) analysis, also referred to as μ analysis, provides a mechanism for determining the stability and performance of a system in the presence of the uncertainties defined in the plant model. The SSV and an equivalent measure, the Multivariable Stability Margin, were introduced in 1982 (Doyle, 1982)(Safonov, 1982). While providing a definition for determining the stability of a system with uncertainties, no closed-form solution exists for finding the SSV or Multivariable Stability Margin. It is possible, however, to calculate reasonably tight bounds on the measure of stability margins. A considerable amount of effort has been placed on reducing the conservative nature of the upper bound, particularly since the method for calculating the bound does not distinguish between real and complex uncertainties. Methods for calculating the actual SSV for real variation in the plant parameters using interative computational techniques (de Gaston and Safonov, 1988) and polynomial methods (Elgersma, Freudenberg and Morton, 1992) exist, but are unwieldly and not suited for most design work. Recent research has also suggested a method for obtaining an uncertainty model which ensures that the number of parametric uncertainties included in the model is a minimal set (Belcastro and Chang, 1992).

H_∞ synthesis provides a method for the design of a controller which minimizes the peak magnitude of the closed-loop frequency response of appropriately modeled systems. The first H_∞ controller design methods were computationally difficult and resulted in controllers having many more states than the plant (Zames, 1981),(Francis, 1987). A breakthrough in 1988 provided a design technique which, similar to

LQG, involves solving two Riccati equations and results in a controller of the same order as the plant (Doyle, Glover, Khargonecker and Francis, 1988). By appropriately defining uncertainties in the model and adding performance weighting functions to the system, it is possible to design a controller using H_∞ synthesis which, when tested using SSV analysis can be shown to be stable and meet performance criteria over all variations quantified in the model. The controller design may fail as mentioned above, however, when the plant model is of high order or there are many uncertainties in the plant. Despite the recent advances in uncertainty analysis and H_∞ synthesis, the problem of finding a controller which is tolerant of these uncertainties still remains.

C. SUMMARY OF THIS WORK

In this dissertation we propose a method for reducing the number of real parametric uncertainties with which the H_∞ control algorithm must contend. The technique involves grouping uncertain parameters which affect the same open loop eigenvalue, then scaling one or more of these to accomodate the effect on the eigenvalue of all the parameter variations. It is then shown that the resulting controller is stable in the presence of all the uncertainties while still meeting the performance criteria.

The remainder of this dissertation is organized as follows. Chapter II provides a summary of robust multivariable control, including the use of the structured singular value for stability analysis and the state-space equations for designing an H_∞ controller. Chapter III introduces sensitivity theory, where we show how parameter uncertainty affects the eigenvalues of the open loop system. The technique for grouping parameters which affect system eigenvalues similarly and scaling one or more of the parameter uncertainties to account for the changes caused by all the variations is demonstrated. This technique is then applied to the design of control systems for

three systems in Chapter IV, a simple four state system and two missile systems. In Chapter V we provide conclusions and suggested areas for further research.

II. ROBUST MULTIVARIABLE CONTROL

Robust multivariable control involves the design of feedback controllers for systems with specified uncertainties which meet established performance and stability criteria. For purposes of this work, we define stability and performance criteria for systems with feedback control as follows (Dailey, 1990):

- **Nominal Stability:** stability of the nominal, unperturbed system.
- **Robust Stability:** stability of the system for a given set of perturbations to the nominal model.
- **Nominal Performance:** the nominal system meets one or more requirements for closed loop performance.
- **Robust Performance:** the system meets performance requirements and remains stable for a given set of perturbations to the nominal model.

A robust H_∞ controller is a feedback controller for which the closed loop plant exhibits robust performance as defined above. The concept of uncertainty in system modeling is presented in Section A. We define a measure of robust stability, the structured singular value, and also introduce performance robustness in Section B. H_∞ control theory and the design of robust H_∞ controllers is described in Sections C and D.

A. UNCERTAINTY

A linear, time invariant model of a physical plant often provides an adequate mathematical representation of the actual system. The model is characterized by

parameters which are chosen to describe the system at a given operating condition, such as when the system is at rest or in an expected steady-state condition. A plant model defined in this way is termed the nominal plant model. In most instances, this nominal model is but one of an infinite number of models required to actually describe the plant at any moment in time. Variations in the plant model from the nominal conditions are manifested in three ways. First, a number of parameters used to describe the nominal plant may be uncertain, or known only within some measurable tolerance. Examples of this are uncertain pole locations or damping factors. Secondly, certain plant dynamics may have been ignored in the nominal design, such as high frequency dynamics. Lastly, parameters of a system may vary as operating conditions of the physical plant change. This is quite common in aircraft and missile control system design, where changes in angle of attack and vehicle weight can dramatically affect the aerodynamic coefficients, which in turn affect the dynamics of the plant. Hereinafter, any of the above manifestations which cause the true plant to vary from the nominal plant will be deemed uncertainties.

1. Unstructured Uncertainty

Consider the plant model shown in Figure 2.1. The actual plant varies from the nominal plant by the uncertainty $\Delta_i(s)$:

$$G(s) = G_o(s)[I + \Delta_i(s)]$$

where $\Delta_i(s)$ represents a frequency dependent uncertainty in the plant dynamics. An uncertainty represented in this manner is termed an *input multiplicative uncertainty* and it can be used by a designer to represent unmodeled dynamics in the plant. To this uncertainty we associate a weighting function which indicates a bound on the magnitude of the uncertainty as a function of frequency. For example the input uncertainty weighting function shown in Figure 2.2 indicates a 50% modeling error in

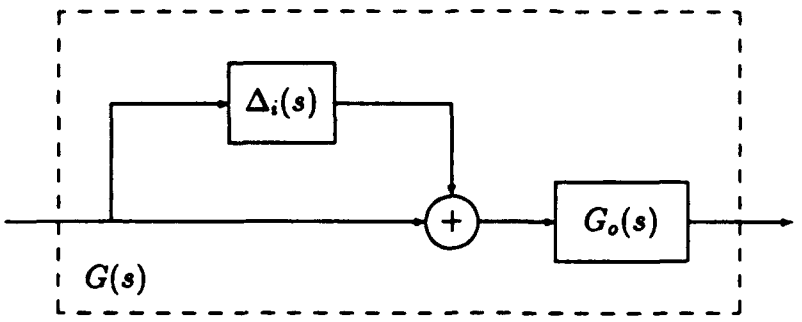

Figure 2.1: System with input multiplicative uncertainty

the plant below 10 rad/sec and a 100% error at 173 rad/sec (Balas, Doyle, Glover, Packard, Smith 1991).

For purposes of our analysis it is convenient to parameterize the uncertainty in a normalized fashion. As a way of illustration, Figure 2.3 shows how the uncertainty $\Delta_i(s)$ is decomposed into a frequency dependent weighting function $W_{\Delta_i}(s)$, indicating the largest singular value at each frequency of the uncertainty, and a normalized uncertainty $\mathbf{\Delta}(s)$ having an infinity norm not exceeding one. The system represented in this way is said to be in standard form, with the plant described by the nominal plant with associated weighting function designated as $P(s)$. The transfer function matrix $P(s)$ now has two inputs, an uncertainty input w_d and an exogenous input w, and two outputs, an uncertainty output y_d and a reference output y. The perturbation block $\mathbf{\Delta}$ can vary in both magnitude and phase, constrained only by $\|\mathbf{\Delta}\|_\infty < 1$. Such an uncertainty is termed an unstructured uncertainty.

Another type of uncertainty is the *input feedback uncertainty*, depicted in Figure 2.4. This type of uncertainty can be used by the designer to provide gain and phase margins in design of the H_∞ controller as described in Appendix C. Both input

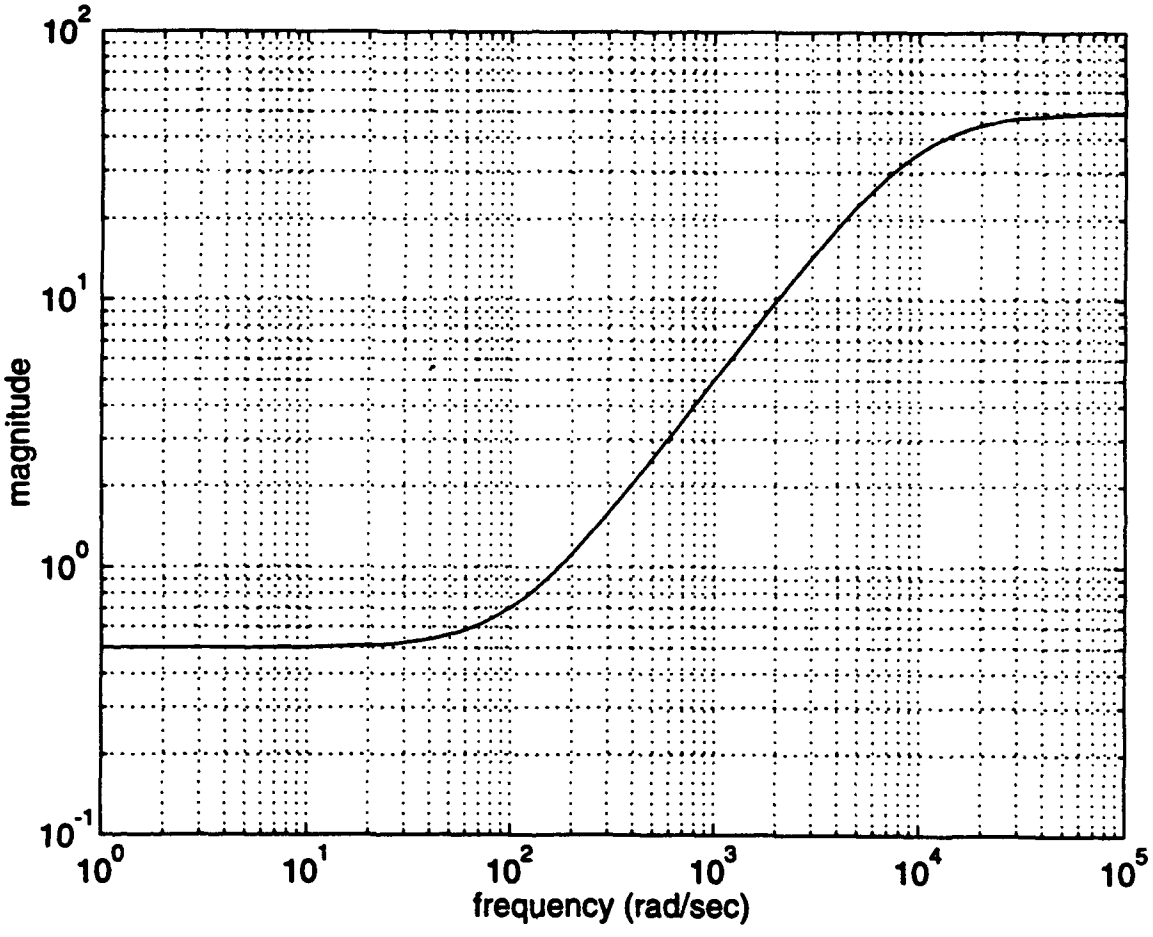

Figure 2.2: Input uncertainty weighting function

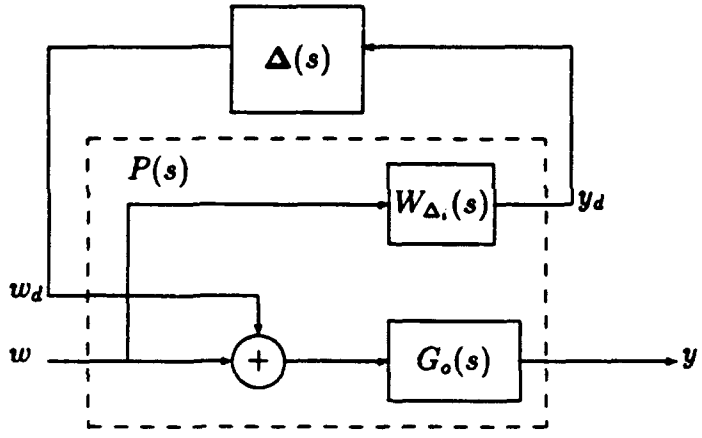

Figure 2.3: Uncertain system in standard form

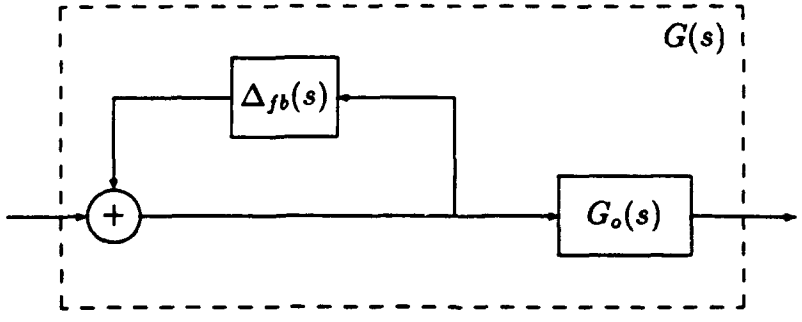

Figure 2.4: System with input feedback uncertainty

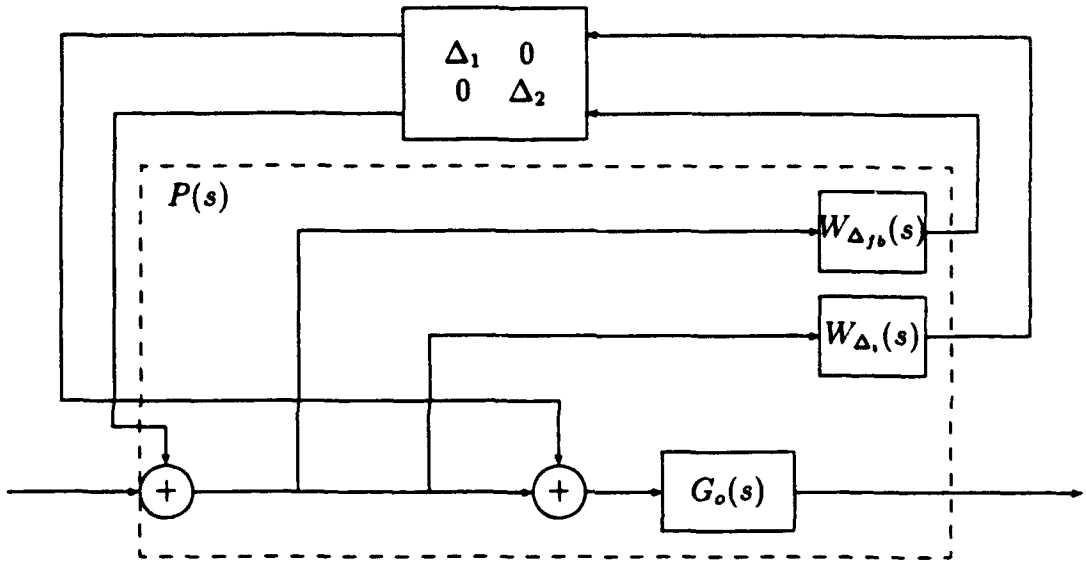

Figure 2.5: Standard form for two uncertainties

multiplicative and feedback uncertainties will appear in the examples of uncertainty reduction in Chapter IV.

2. Structured Uncertainty

Figure 2.5 shows a feedback uncertainty in standard form combined with an input multiplicative uncertainty. The perturbation block $\mathbf{\Delta}$ now has two blocks along the diagonal, Δ_1 and Δ_2, with scaling provided such that $\|\mathbf{\Delta}\|_\infty \leq 1$. In this structure, the perturbation block is no longer free to vary in all elements, as the off diagonal blocks are now zero. Two or more uncertainties presented in this way become structured uncertainties. An unstructured uncertainty is a special case of structured uncertainty, where the perturbation consists of only one block.

The uncertainties presented above describe very general variations in the system transfer function. Very often, however, the designer has some knowledge about the specific variations of the parameters in the plant model. The tolerance to which the parameters have been mearsured may be known or the parameters may vary in some prescribed manner according to the operating conditions. These

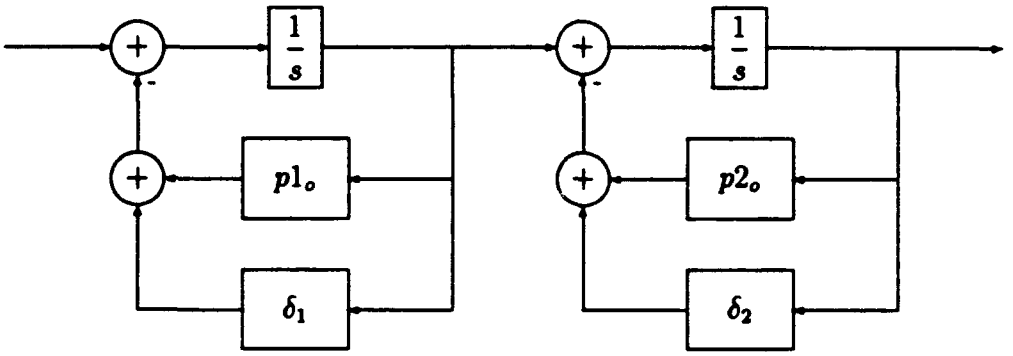

Figure 2.6: System with parametric uncertainty

uncertainties, characterized by real scalar variations of certain parameters, are termed parametric uncertainties.

As an example, Figure 2.6 shows a two state system with uncertainties in the pole locations $p1_o$ and $p2_o$. The uncertainties δ_1 and δ_2 are defined to lie in some region constrained by $\delta_1 \in [-\epsilon_1, +\epsilon_1]$ and $\delta_2 \in [-\epsilon_2, +\epsilon_2]$. The same system is shown in its standard form in Figure 2.7. Although the uncertainties δ_1 and δ_2 are real scalars, the perturbation block $\mathbf{\Delta}$ is restricted only by its diagonal structure and infinity norm; Δ_1 and Δ_2 may take on complex values. The design and analysis techniques presented in this chapter do not distinguish between real and complex perturbations, therefore real parameter uncertainties are treated as being complex valued. It is this assumption of complex blocks in the perturbation matrix which will subsequently allow us to reduce the number of parametric uncertainties needed for a robust controller design.

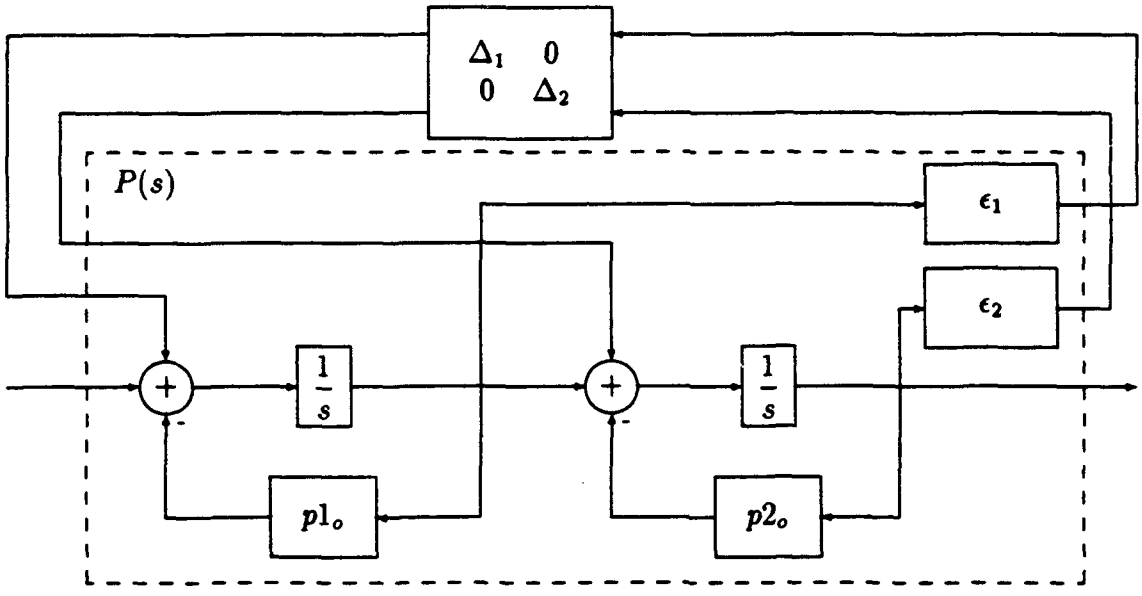

Figure 2.7: Parametric uncertainty in block diagonal form

B. ROBUST STABILITY

A nominally stable feedback system can become unstable in the presence of uncertainties in the nominal plant model. When designing feedback systems, we need a stability measure other than just stability of the nominal system, and therefore introduce the concept of robust stability as a measure of a system's stability in the presence of uncertainties in the plant. In this section we will define a measure of robust stability and describe the method used for its determination.

1. Stability Robustness

Consider the system in Figure 2.8 showing the uncertainty block Δ. The plant $P(s)$ contains the nominal plant and uncertainty weightings such that $\|\Delta(s)\|_\infty \leq 1$. Associated with the system is a feedback controller $K(s)$ designed on the basis of the nominal plant to meet given specifications. The inputs to $P(s)$, w_d, w and u are the uncertainty inputs, exogenous inputs, and control inputs, respectively. The outputs y_d, y and m are the uncertainty outputs, reference outputs and measurements, respectively.

By combining $P(s)$ and $K(s)$ into a single block $M(s)$, the system can be represented as in Figure 2.9, with its transfer function $M(s)$ partitioned as

$$\begin{bmatrix} y_d \\ y \end{bmatrix} = \begin{bmatrix} M_{11}(s) & M_{12}(s) \\ M_{21}(s) & M_{22}(s) \end{bmatrix} \begin{bmatrix} w_d \\ w \end{bmatrix}$$

Since the compensator for the system, $K(s)$, is designed for the nominal plant, the system $M(s)$ is nominally stable. To guarantee that the closed loop system will remain stable, we need only show that the loop containing the perturbation matrix is stable for all perturbations. Due to the normalization of the perturbation matrix Δ, only the transfer function from w_d to y_d, namely $M_{11}(s)$, need be analyzed. Using the stability analysis results from Appendix B, a sufficient condition for robust stability

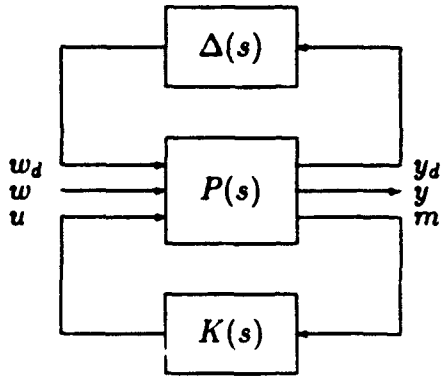

Figure 2.8: Standard form for an uncertain system with feedback control

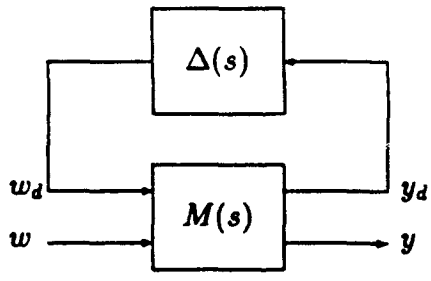

Figure 2.9: Model for robust analysis

for all $\Delta \in \mathbf{\Delta}$ such that $\|\mathbf{\Delta}\|_\infty \leq 1$ is

$$\|M_{11}\|_\infty < 1. \tag{2.1}$$

We observe, however, that the only constraint this result places on the perturbation matrix is a bound on the infinity norm; off diagonal elements are free to assume a non-zero value. As presented earlier, though, the perturbation matrix for structured uncertainties is actually block diagonal. The stability criterion in Equation 2.1 is thus too conservative (Doyle, 1982). In the next section, we will exploit the structure of the perturbation matrix and develop a less conservative criterion for robust stability.

2. The Structured Singular Value

An alternative to Equation 2.1 for determining robust stability can be deduced from Figure 2.9. Stability in the loop containing the perturbation requires that for all frequencies

$$\det\{I + M\Delta\} \neq 0 \quad \text{for all } \Delta \in \mathbf{\Delta} \tag{2.2}$$

where $\mathbf{\Delta}$ is the set of all possible perturbation matrices. Doyle has defined a function which can be used to define the necessary and sufficient conditions for stability, the Structured Singular Value (SSV), $\mu(M)$ (Doyle, 1982). When Equation 2.2 holds, this function has the property

$$\bar{\sigma}(\Delta)\mu(M) < 1 \tag{2.3}$$

where $\bar{\sigma}(\Delta)$ is the maximum singular value of the perturbation matrix Δ. The SSV is defined as

$$\mu(M) = \begin{cases} 0 & \text{if no } \Delta \in \mathbf{\Delta} \text{ solves } \det(I + M\Delta) = 0 \\ \{\min_{\Delta \in \mathbf{\Delta}}(\bar{\sigma}(\Delta) \mid \det(I + M\Delta) = 0)\}^{-1} & \text{otherwise} \end{cases}$$

It can be shown that the SSV has the following properties (Doyle, 1982):

1. $\mu(\alpha M) = \mid \alpha \mid \mu(M)$
2. $\mu(I) = 1$
3. $\mu(AB) \leq \bar{\sigma}(A)\mu(B)$ $\quad A, B$ complex matrices
4. $\mu(\Delta) = \bar{\sigma}(\Delta)$
5. $D\Delta D^{-1} = \Delta \quad \forall\, D \in \mathcal{D}$
6. $\mu(DMD^{-1}) = \mu(M)$ $\quad D$ a nonsingular diagonal matrix
7. $\max \rho(UM) \leq \mu(M) \leq \inf_{D \in \mathcal{D}} \bar{\sigma}(DMD^{-1})$

where $\rho(X)$ is the spectral radius, or largest eigenvalue, of X and the two sets $\mathcal{D}$ and $\mathcal{U}$ are defined as

$$\begin{aligned} \mathcal{D} &= \text{diag}(d_1 I_{k_1}, d_2 I_{k_2}, \ldots, d_n I_{k_n}),\ d_i \in \mathcal{R}; \\ \mathcal{U} &= \text{diag}(U_1, U_2, \ldots, U_n), \mid U_i \in \mathcal{C}^{k_i \times k_i},\ U_i^* U_i = I_{k_i}. \end{aligned}$$

and I_k is the $k \times k$ identity matrix. Unfortunately, the SSV cannot be analytically determined from its definition. Numerical methods for computing the SSV exist, however they are extremely cumbersome and not appropriate for most design work (de Gaston and Safonov, 1988). We shall therefore use Property 7 and calculate the bounds for the SSV. These bounds are used in design and analysis in place of the actual SSV.

a. Calculating bounds for the SSV

Property 7 above provides upper and lower bounds for the SSV. Doyle (Doyle, 1982) has proven that the lower bound of μ, given by

$$\max_{U \in \mathcal{U}} \rho(MU) \leq \mu(M) \tag{2.4}$$

is actually an equality. This problem is not convex, however, and local maxima can exist. The upper bound for μ is given as

$$\mu(M) \leq \inf_{D \in \mathcal{D}} \bar{\sigma}(DMD^{-1}). \tag{2.5}$$

Determining this bound is a convex optimization problem and it has one minimum which has to be the global minimum. The minimum value of $\bar{\sigma}(DMD^{-1})$ can be efficiently computed using one of several optimization algorithms. This upper bound has been found to be generally tight, usually within 5% to 15% of the SSV. In the remainder of this dissertation, we will use the SSV, or "mu" to describe the bound defined by Equation 2.5. The actual value of $\mu(M)$, when needed, will hereinafter be referred to as the real μ.

3. Performance Robustness

A number of performance criteria can be defined by bounding $\|T_{yw}\|_\infty$, where T_{yw} is the transfer function from the set of exogenous inputs w to the set of error measurements y. By appropriately weighting the output vector y, we define the performance criterion such that it is bounded by

$$\|T_{yw}\|_\infty < 1 \tag{2.6}$$

when the desired performance requirements are met (Bibel and Malyevac, 1992). A system is said to possess nominal performance if the bound in Equation 2.6 is satisfied for the nominal plant. The system is said to possess robust performance if the system remains stable and meets the performance criteria in the presence of all uncertainties. Robust performance requirements can be included in SSV analysis by adding a block Δ_p as a diagonal term of the uncertainty matrix Δ, as shown in Figure 2.10. The reason why we take this approach is because, in this way, robust performance and robust stability can be addressed within the same framework. The

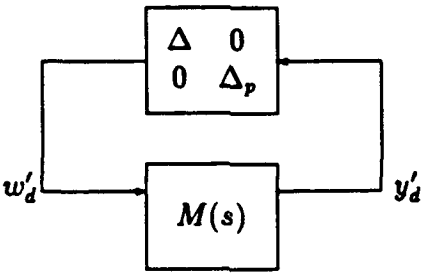

Figure 2.10: Model for robust performance

performance block $\Delta_p \in C^{r \times q}$, where r is the number of exogenous inputs and q is the number of error measurements. The augmented uncertainty inputs and outputs for the plant are now defined by

$$w'_d = \begin{bmatrix} w_d \\ w \end{bmatrix}$$

$$y'_d = \begin{bmatrix} y_d \\ y \end{bmatrix}$$

Expressed in this form, the test for robust performance now involves computing the SSV for the entire system $M(s)$, rather than just $M_{11}(s)$ as in the case of robust stability. The system will therefore exhibit robust performance provided that $\mu(M) < 1$. It is worth noting that performance robustness is a more stringent test than stability robustness.

C. H_∞ CONTROL THEORY

The use of H_∞ control theory to design a feedback controller for a multi-input multi-output plant is introduced in this section. H_∞ design involves minimizing

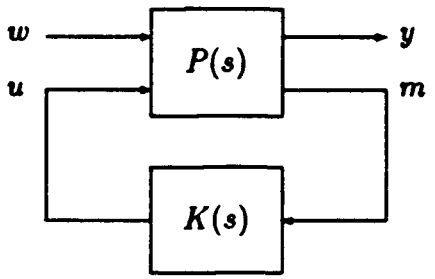

Figure 2.11: Model for H_∞ controller design

the peak value of the frequency response magnitude of selected closed-loop transfer functions. The efficacy of the resulting design in the presence of uncertainties and performance criteria is then analyzed using the techniques described in the preceding sections.

1. H_∞ Optimization

Consider the system shown in Figure 2.11. The variables are defined as follows:

- $w \in \mathcal{R}^{m_1}$ is the input disturbance vector, including uncertainty inputs, reference inputs and disturbances,
- $u \in \mathcal{R}^{m_2}$ is the control vector generated by the controller,
- $y \in \mathcal{R}^{p_1}$ is the error vector containing those signals we desire to minimize,
- $m \in \mathcal{R}^{p_2}$ is the measurement vector, and input to the controller.

Since the system is assumed to be linear time invariant, by partitioning the plant $P(s)$ we can write the outputs in terms of the inputs as

$$\begin{bmatrix} y \\ m \end{bmatrix} = P(s) \begin{bmatrix} w \\ u \end{bmatrix} = \begin{bmatrix} P_{11}(s) & P_{12}(s) \\ P_{21}(s) & P_{22}(s) \end{bmatrix} \begin{bmatrix} w \\ u \end{bmatrix}$$

or, equivalentl,

$$\begin{aligned} y &= P_{11}w + P_{12}u \\ m &= P_{21}w + P_{22}u \end{aligned}$$

Under closed loop conditions where $u = Km$, we can relate the disturbance w to the error signal y as

$$y = [P_{11} + P_{12}K(I - P_{22}K)^{-1}P_{21})]w = \mathcal{F}_l(P, K)w.$$

where $\mathcal{F}_l(P, K)$ is termed the lower linear fractional transformation of (P, K). Using the above definitions for w and y, it is possible to put a number of design problems into the form

$$\text{minimize } \|\mathcal{F}_l(P, K)\|_\infty \tag{2.7}$$

This is the H_∞-optimization problem.

2. Solution of the H_∞ optimization problem

A state-space solution to Equation 2.7 is summarized here (Doyle, Glover, Khargonekar and Francis, 1988). The system in Figure 2.11 can be described in state space form as

$$\begin{aligned} \dot{x}(t) &= Ax(t) + B_1w(t) + B_2u(t), \\ y(t) &= C_1x(t) + D_{11}w(t) + D_{12}u(t), \\ m(t) &= C_2x(t) + D_{21}w(t) + D_{22}u(t). \end{aligned}$$

All uncertainty and performance function weights are assumed to be included in this plant. The plant $P(s)$ now has a transfer function which can be expressed in matrix form as

$$P(s) = \begin{bmatrix} D_{11} & D_{12} \\ D_{21} & D_{22} \end{bmatrix} + \begin{bmatrix} C_1 \\ C_2 \end{bmatrix} (sI - A)^{-1} [B_1 \quad B_2].$$

For convenience, the plant is often symbolically expressed as

$$P(s) = \left[\begin{array}{c|cc} A & B_1 & B_2 \\ \hline C_1 & D_{11} & D_{12} \\ C_2 & D_{21} & D_{22} \end{array}\right]$$

which is not a transfer function matrix, but rather a compact way of expressing $P(s)$. The minimization called for in Equation 2.7 has no convenient closed form solution, so we will instead solve a related problem and find a controller such that

$$\|\mathcal{F}_l(P, K)\|_\infty < \gamma, \quad \gamma \in \mathcal{R} \tag{2.8}$$

where γ is a predetermined parameter. This will involve solving two Riccati equations requiring the following constraints on the system $P(s)$:

1. (A, B_2, C_2) is stabilizable and detectable.
2. rank $D_{12} = m_2$; rank $D_{21} = p_2$.
3. $D_{12}^T D_{12} = I$; $D_{21} D_{21}^T = I$; (For D_{12} and D_{21} full rank, scaling can be used to make this constraint true.)
4. $D_{11} = 0$; $D_{22} = 0$.
5. rank $\begin{bmatrix} A - j\omega I & B_2 \\ C_1 & D_{12} \end{bmatrix} = n + m_2 \quad \forall\, \omega \in \mathcal{R}$
6. rank $\begin{bmatrix} A - j\omega I & B_1 \\ C_2 & D_{21} \end{bmatrix} = n + p_2 \quad \forall\, \omega \in \mathcal{R}$

Denoting the solution to the algebraic Riccati equation $A^TX + XA - XRX + Q = 0$ in the Hamiltonian matrix form

$$X = \mathrm{Ric}\begin{bmatrix} A & -R \\ -Q & -A^T \end{bmatrix},$$

we now define two matrices X_∞ and Y_∞ as the solutions to

$$X_\infty = \mathrm{Ric}\begin{bmatrix} A & \gamma^{-2}B_1B_1^T - B_2B_2^T \\ -C_1^TC_1 & -A^T \end{bmatrix} \tag{2.9}$$

and

$$Y_\infty = \mathrm{Ric}\begin{bmatrix} A^T & \gamma^{-2}C_1^TC_1 - C_2^TC_2 \\ -B_1B_1^T & -A \end{bmatrix} \tag{2.10}$$

Defining three intermediate terms

$$\begin{aligned} Z &= (I - \gamma^{-2}YX)^{-1}; \\ F &= -B_2^TX; \\ L &= -YC_2^T, \end{aligned}$$

the state-space form of the controller $K(s)$

$$\begin{aligned} \dot{x}_c(t) &= A_cx_c(t) + B_cm(t) \\ u(t) &= C_cx_c(t) \end{aligned}$$

is defined by the matrices

$$\begin{aligned} A_c &= A + \gamma^{-2}B_1B_1^TX + B_2F + ZLC_2; \\ B_c &= -ZL; \\ C_c &= F. \end{aligned}$$

The following conditions must be met for a compensator K satisfying Equation 2.8 to exist:

1. The solution to Equation 2.9, X_∞, is positive semidefinite and the associated Hamiltonian has no imaginary eigenvalues.

2. The solution to Equation 2.10, Y_∞, is positive semidefinite and the associated Hamiltonian has no imaginary eigenvalues.

3. The spectral radius $\rho(X_\infty Y_\infty) < \gamma^2$.

The controller that minimizes the cost function in Equation 2.8 is found by iteratively reducing γ, with the initial value selected large enough to meet the above criteria. The value of γ is reduced using the bisection method until no improvement in γ is acheived (Doyle, Glover, Khargonekar and Francis, 1988). A method for finding the minimum value of γ without iteration has been suggested by Chen, Saberi and Ly (Chen, Saberi and Ly, 1992).

D. D-K ITERATION

The design of an H_∞ controller using the procedure of the previous section does not imply robust stability or performance. The algorithm generates a controller which only guarantees stability of the nominal closed loop system and minimizes $\|\mathcal{F}_l(P,K)\|_\infty$. The resulting closed loop system must still be tested for performance robustness as described in Section B. If the resultant structured singular value is not less than one, the system must be modified and another controller designed. We now introduce the technique for designing a closed loop system that has performance robustness. This technique uses H_∞ control design on an augmented plant and iteratively modifies the plant with frequency dependent weighting functions.

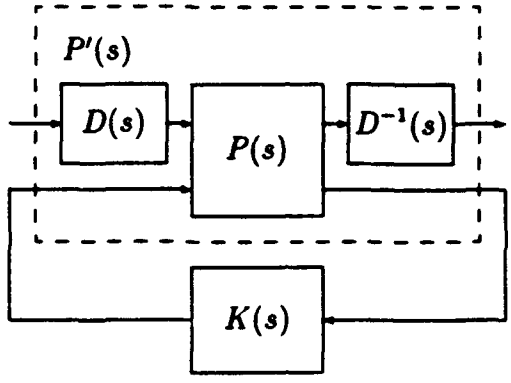

Figure 2.12: Model for D-K iteration

1. Modifying the Plant With D-Scales

Recalling from Equation 2.5 that the actual measure of robustness is the SSV and not the maximum singular value, the problem stated in Equation 2.7 can be more accurately posed as

$$\text{minimize } \|D\mathcal{F}_l(P,K)D^{-1}\|_\infty \tag{2.11}$$

where $D = D(s)$ is a frequency dependent, nonsingular diagonal scaling function matrix. It can be shown that in this way we attempt to minimize the SSV rather than the maximum singular value (Dailey, 1990).

The appropriate D-scales are selected in the same manner as in the Structured Singular Value problem and appended to the plant as shown in Figure 2.12. A new H_∞ controller is then designed for the augmented plant and tested for robustness. This process of controller design, robustness testing and D-scale augmentation is called D-K iteration and continues until the maximum value of the SSV is less than one or no further reduction is possible. If the iteration procedure does not succeed

in designing a robust controller, the uncertainty weights or performance criteria in the plant $P(s)$ must be modified and the above design process repeated.

III. PARAMETRIC UNCERTAINTY REDUCTION

The concept of plant uncertainty has been introduced in Chapter II. As mentioned in Chapter I, current H_∞ synthesis techniques may fail to design a robust controller when all the known uncertainties are included in the plant model. In this chapter we present a technique for reducing the number of parametric uncertainties used in the design of a robust H_∞ controller. This reduction is accomplished by using sensitivity theory to identify groups of parameters whose variations affect the same open loop plant eigenvalues, and then quantifying their effect on the eigenvalues. The variation in one or more of these parameters is then scaled in a manner which causes the same effect on the eigenvalue when acted upon by all the uncertainties. An H_∞ controller is designed for the system with the reduced number of uncertainties and tested for robustness with the system containing the original uncertainties.

Sensitivity theory and the procedure for quantifying the effects of parameter variation on the eigenvalues of the open loop system is described in Section A. A technique for reducing the number of uncertainties used for designing a robust H_∞ controller is presented in Section B.

A. SENSITIVITY THEORY

In this section we present a discussion introduced by Frank (Frank, 1978) of the effect of real parametric uncertainties on the nominal plant. We will be most concerned with the effect the parameter variations have on the system eigenvalues. The approach taken will be based on sensitivity theory by developing an appropriate sensitivity function. This function, not to be confused with the sensitivity transfer

function of the closed loop system, relates the change in the parameter of interest to specific characteristics of the plant. We first present the underlying theory in general form and then define the sensitivity function relating changes in plant parameters to changes in the open loop eigenvalues.

1. General Discussion

Let the parameters which describe a system be represented by a vector $\alpha = [\alpha_1, \alpha_2, \ldots, \alpha_m]^T$. The parameter vector is uncertain around a nominal vector α_o, which can be written as

$$\alpha = \alpha_o + \Delta\alpha. \tag{3.1}$$

For linear, time invariant systems, the plant and input matrices are a function of α, e.g.,

$$\dot{x} = A(\alpha)x + B(\alpha)u. \tag{3.2}$$

We now introduce a general function, $\xi = \xi(\alpha)$, which characterizes some behavior of the system, for example a performance index, set of eigenvalues or the state of the system.

Defining the nominal system function by $\xi_o \equiv \xi(\alpha_o)$, the absolute sensitivity function is defined by

$$S^{\xi}_{\alpha_i} \equiv \frac{\partial \xi(\alpha)}{\partial \alpha_i}\Big|_{\alpha_o} \equiv S^{\xi}_{\alpha_i}(\alpha_o) \quad i = 1, 2, \ldots, m \tag{3.3}$$

with $S^{\xi}_{\alpha_i}$, $i = 1, 2, \ldots, m$ relating the change in ξ to a change in each parameter α_i. For small perturbations, the total perturbation of ξ due to changes in α is computed as

$$\Delta\xi = \sum_{i=1}^{m} S^{\xi}_{\alpha_i} \Delta\alpha_i. \tag{3.4}$$

We next discuss the method for determining the Sensitivity Function.

a. Calculating the sensitivity function

The plant parameter vector α contains elements which can be functions of time varying parameters themselves, such as mass, angle of attack, etc. The element α_i can then be represented as $\alpha_i \equiv \alpha_i(p_1, p_2, \ldots, p_r)$, with the nominal vector denoted by p_o. The goal now is to derive the sensitivity function for ξ based on changes in p:

$$S^{\xi}_{p_j} = \frac{\partial \xi}{\partial p_j}\Big|_{p_o}, \quad j = 1, 2, \ldots, r \tag{3.5}$$

Applying the chain rule, we can write

$$\frac{\partial \xi}{\partial p_j} = \frac{\partial \xi}{\partial \alpha_1}\frac{\partial \alpha_1}{\partial p_j} + \frac{\partial \xi}{\partial \alpha_2}\frac{\partial \alpha_2}{\partial p_j} + \ldots + \frac{\partial \xi}{\partial \alpha_m}\frac{\partial \alpha_m}{\partial p_j}, \quad j = 1, 2, \ldots, r. \tag{3.6}$$

Evaluating this at $\alpha_o = \alpha(p_o)$, and using the definition of $S^{\xi}_{\alpha_i}(\alpha_o)$ in Equation 3.3, Equation 3.5 now becomes

$$S^{\xi}_{p_j} = \sum_{i=1}^{m} S^{\xi}_{\alpha_i}\frac{\partial \alpha_i(p)}{\partial p_j}\Big|_{p_o}, \quad j = 1, 2, \ldots, r \tag{3.7}$$

and the total parameter-induced uncertainty can be expressed as

$$\Delta\xi = \sum_{j=1}^{r}\sum_{i=1}^{m} S^{\xi}_{\alpha_i}\frac{\partial \alpha_i}{\partial p_j}\Big|_{p_o} \cdot \Delta p_j \tag{3.8}$$

The quantity $\partial\alpha_i/\partial p_j$ must be defined for each choice of the parameter vectors α and p. In the next section, Equation 3.8 is applied to the eigenvalue sensitivity problem.

2. Eigenvalue Sensitivity

We now consider the case where ξ is the eigenvalues of the system and $\alpha = a_{ij}$ the elements of the plant matrix in Equation 3.2. We define the eigenvector sensitivity as follows:

Given an LTI system with dynamics defined by Equation 3.2 with $A = A(a_{ij})$, $A \in \mathcal{R}^{n \times n}$ and a_{ij} the elements of the matrix A having eigenvalues λ_k, the

sensitivity function relating perturbations in the eigenvalues to perturbations in the elements a_{ij} is given by

$$S_{a_{ij}}^{\lambda_k} \equiv \frac{\partial \lambda_k}{\partial a_{ij}} |_{A(a_o)} \tag{3.9}$$

where a_o represents the nominal values of the matrix A.

To develop a method of computing this sensitivity function, we first define the right and left eigenvectors v_i and w_i associated with the eigenvalue λ_i of the system described in Equation 3.2. The right eigenvectors v_i, $(i = 1, 2, \ldots, n)$ are defined by $Av_i = \lambda_i v_i$ and the left eigenvectors w_i, $(i = 1, 2, \ldots, n)$ by $A^T w_i = \lambda_i w_i$. Letting Λ equal the diagonal matrix of eigenvalues λ_i and defining $v = [v_1, v_2, \ldots, v_n]$ and $w = [w_1, w_2, ldots, w_n]$, the matrix form of the eigenvector relations become

$$\Lambda = \begin{bmatrix} \lambda_1 & & \\ & \ddots & \\ & & \lambda_n \end{bmatrix}$$

$$Av = v\Lambda$$

$$A^T w = w\Lambda$$

The right and left eigenvectors are normalized such that $w^T v = v^T w = I$ where I is the identity matrix. Using the above equations, we can now write Λ as

$$\Lambda = w^T A v.$$

It can be shown that the sensitivity matrix $S_{a_{ij}}^{\lambda_k}$ is directly related to the left and right eigenvectors as

$$S_{a_{ij}}^{\lambda_k} \equiv \frac{\partial \lambda_k}{\partial a_{ij}} = w_k v_k^T, \quad i, j, k = 1, 2, \ldots, n \tag{3.10}$$

We now describe the method for determining the term $\partial a_{ij}/\partial p$. We define a perturbed parameter vector

$$p^1 = [p_1 + \Delta p_1, p_2 + \Delta p_2, \ldots, p_r + \Delta p_r]$$

For small perturbations around the nominal vector, $\partial a_{ij}/\partial p$ can be approximated by $\Delta a_{ij}/\Delta p$. The terms Δa_{ij} are the elements of the matrix

$$\Delta A = A(a_o) - A(a)$$

where $a = a(p^1)$.

For one parameter variation, $\Delta p = \Delta p_l$, and $\Delta a_{ij}/\Delta p = \Delta a_{ij}/\Delta p_l$. The chain rule is used to find the eigenvalue sensitivity $\partial \lambda_k/\partial p_l$

$$\frac{\partial \lambda_k}{\partial p_l} = \sum_{i=1}^{n}\sum_{j=1}^{n} \frac{\partial \lambda_k}{\partial a_{ij}} \cdot \frac{\partial a_{ij}}{\partial p_l}, \quad k = 1,2,\ldots,n \quad l = 1,2,\ldots,r \tag{3.11}$$

Recognizing $\partial \lambda_k/\partial a_{ij}$ as the eigenvalue sensitivity function from Equation 3.10 and assuming small perturbations, Equation 3.11 becomes

$$\frac{\Delta \lambda_k}{\Delta p_l} = \sum_{i=1}^{n}\sum_{j=1}^{n} S_{a_{ij}}^{\lambda_k} \cdot \frac{\Delta a_{ij}}{\Delta p_l}, \quad l = 1,2,\ldots,r \tag{3.12}$$

This equation provides a numerical method for determining the sensitivity of each eigenvalue to any parameter in the system. In the next section we will investigate the problem of changes in the eigenvalues and present the procedure for dealing with perturbations not infinitesimally small. A two state example will be presented which uses the methods described in this chapter to calculate eigenvalue sensitivity.

B. UNCERTAINTY REDUCTION

The theory for calculating the sensitivity of system eigenvalues to small variations in plant parameters was derived in the previous section. Not all the system parameters, however, affect the eigenvalues. In this chapter we deal only with those parameters that affect the eigenvalues of the open loop system, and the example in this section will illustrate that each parameter typically affects only a small number of eigenvalues. We will show that by grouping parameters that affect the same eigenvalue, a single parameter can be scaled and used in the controller design to

accommodate all the uncertainties of the grouped parameters. In subsection 1 the effects of parameter variations on the eigenvalues are illustrated, and the case of large perturbations will be included. In subsection 2 an example is presented which incorporates the techniques previously developed.

1. Calculating the Eigenvalue Sensitivity

In Section A, the sensitivity of the k_{th} eigenvalue of a system, λ_k, to variations in a single parameter p_l was defined in Equation 3.12. In order to select an appropriate parameter for scaling, we first describe the manner in which parameter variations affect pole locations, showing that the maximum eigenvalue change will occur for some combination of the maximum parameter variations. Procedures for dealing with perturbations large enough that the Sensitivity Function changes significantly over the parameter variation, which is often the case, will be discussed next.

a. Behavior of eigenvalues

In this section we consider the perturbation of a single real eigenvalue or a pair of complex eigenvalues. First, consider one eigenvalue of a system in the complex plane. The eigenvalue is determined by the equation

$$\lambda + \alpha = 0$$

where $\alpha = \alpha(p)$, the parameter vector of the system. The variation in the pole location is

$$\Delta\lambda = -\Delta\alpha \tag{3.13}$$

where $\Delta\alpha = \alpha(p_o) - \alpha(p_o + \Delta p)$. Figure 3.1 describes a one state system with two uncertain parameters, $P = P_o + \Delta P$ and $K = K_o + \Delta K$. The characteristic equation

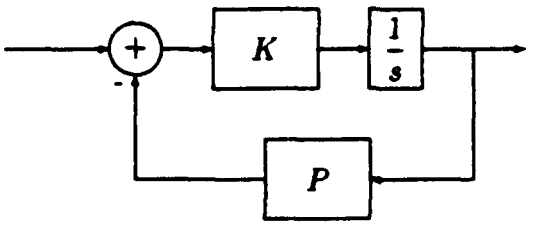

Figure 3.1: Uncertain one state system

of this system is

$$\lambda + P K = 0. \tag{3.14}$$

From Equation 3.14, it is apparent that the maximum eigenvalue change will occur for some combination of the maximum parameter perturbations.

In the case of complex roots, the eigenvalues are the solutions to

$$\lambda^2 + \beta\lambda + \gamma = 0 \tag{3.15}$$

where $\beta = \beta(p)$ and $\gamma = \gamma(p)$. The relationship between the parameter variations and $\Delta\lambda$ is best illustrated by an example. Consider an uncertain system with complex eigenvalues as shown in Figure 3.2. For the time being, the eigenvalues are assumed to remain complex over the full range of parameter variations. (This constraint will be removed later.) In this particular case, the characteristic equation of the system is given by

$$\lambda^2 + P_1\lambda + P_2 = 0 \tag{3.16}$$

with roots

$$\lambda_{1,2} = \frac{-P_1 \pm \sqrt{P_1^2 - 4 \cdot P_2}}{2} \tag{3.17}$$

The variation in the real part of the pole is due entirely to variations in P_1. The variation in the imaginary part of the eigenvalue is due to variations in both P_1 and

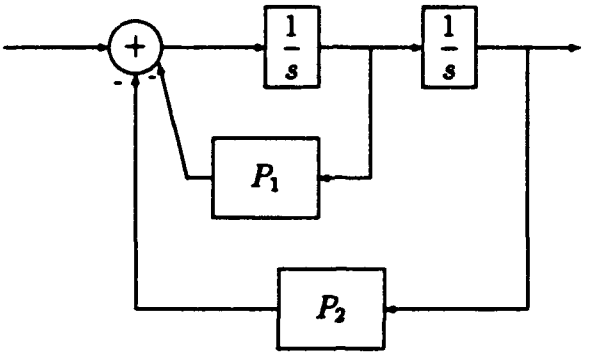

Figure .2: Uncertain two state system

P_2. Note that variations in P_2 only affect the imaginary part of the eigenvalue. From Equation 3.17, it is clear that as with a purely real pole, the maximum eigenvalue change will again occur for some combination of the maximum parameter variations. It will also be shown that the sensivity to change depends on the direction in which we move the pole, and in some instances the sensitivity remains constant throughout the change.

In general, most physical systems will be found to have parameter variations large enough that the eigenvalue sensitivity will vary considerably over the entire range of values. In uncertainty reduction we will be most concerned with the maximum change of the eigenvalue, which occurs at the extreme of the parameter variations. In practice, sensitivities for all parameters are calculated first for the nominal case. Sensitivities for the maximum perturbation case are calculated only for a select number of parameters, as described in the following section, where we also show that the point of maximum eigenvalue sensitivity will be of the most interest.

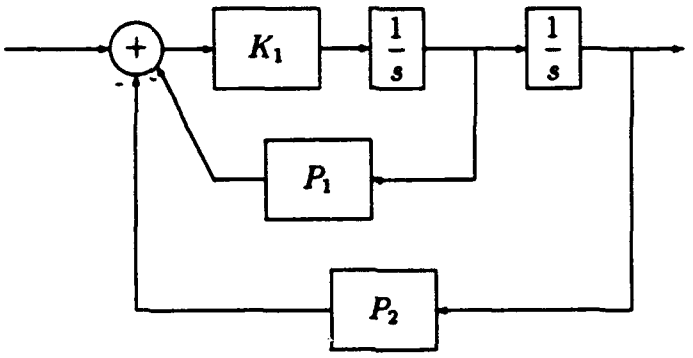

Figure 3.3: Two state system with three uncertain parameters

2. Uncertainty Reduction

We will now detail the steps necessary to determine the eigenvalue sensitivity, group parameters affecting the same eigenvalues and scale a parameter variation to accommodate the maximum change in pole location. To illustrate, let us consider a numerical example. The uncertain two state system shown in Figure 3.3 is characterized by the parameters $P1$, $P2$, and $K1$, where

$$\begin{aligned} P1 &= P1_o + \delta_{P1} \\ P2 &= P2_o + \delta_{P2} \\ K1 &= K1_o + \delta_{K1} \end{aligned}$$

The nominal parameters and associated uncertainties are

$$\begin{aligned} P1_o &= 8 \\ P2_o &= 2 \\ K1_o &= 100 \\ \delta_{P1} &\in [-0.4 \cdot P1_o, +0.4 \cdot P1_o] \end{aligned}$$

TABLE 3.1: EIGENVALUE SENSITIVITY

		Eigenvalue Sensivitivy	
Parameter	Evaluated at	$\Delta\lambda/\Delta p$	$\mid \Delta\lambda/\Delta p \mid$
p1	$p1_o$	$-50 \pm j28.5$	57.3
	$p1_o + \Delta p1_{max}$	$-50 \pm j48.1$	69.3
	$p1_o - \Delta p1_{max}$	$-50 \pm j15.6$	52.4
p2	$p2_o$	$0 \mp j4.1$	4.1
	$p2_o + \Delta p2_{max}$	$0 \mp j3.3$	3.3
	$p2_o - \Delta P2_{max}$	$0 \mp j5.9$	5.9
k1	$k1_o$	$-0.07 \mp j0.04$	0.080
	$k1_o + \Delta k1_{max}$	$-0.07 \mp j0.03$	0.076
	$k1_o - \Delta k1_{max}$	$-0.07 \mp j0.05$	0.088

$$\delta_{P2} \in [-0.4 \cdot P2_o, +0.4 \cdot P2_o]$$

$$\delta_{K1} \in [-0.2 \cdot K1_o, +0.2 \cdot K1_o]$$

The pole locations for the nominal system are shown in Figure 3.4, along with the pole motions for the above parameter variations. Note that the variations in $P1$ and $K1$ result in real and imaginary perturbation of the pole locations, while the variation in $P2$ results in purely imaginary motion of the poles. (This is consistent with Equation 3.17.)

Using the techniques described in Section A, the eigenvalue sensitivities from Equation 3.12 for nominal and maximum perturbation cases are listed in Table 3.1. It is easy to see how the sensitivity changes as the parameters vary.

As discussed in Chapter 2, the parametric uncertainties can be arranged in a block matrix as shown in Figure 3.5. The perturbation block Δ has real scalar values on the diagonal and all other elements equal to zero. The only restriction placed on the perturbation block by the H_∞ control algorithm, however, is that the frequency response have a bounded infinity norm. The elements in Δ, although real, may in practice assume complex values without affecting the controller design process. Without loss of generality, then, we can express each element in Δ as a bounded

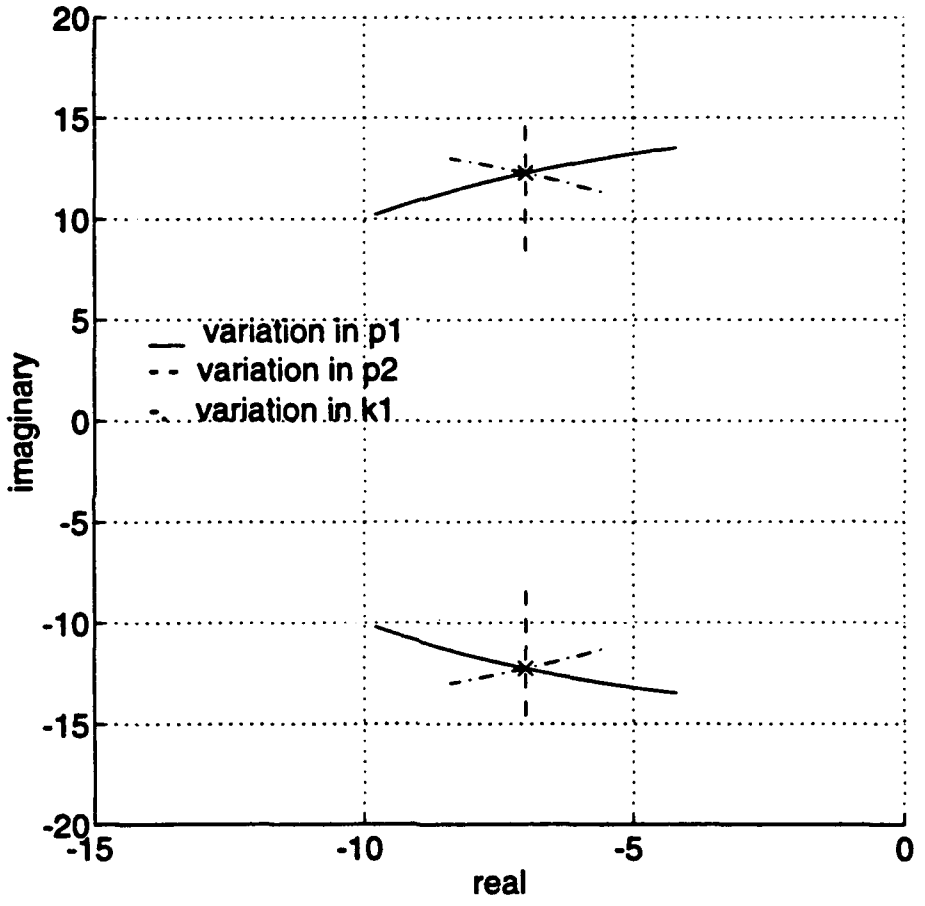

Figure 3.4: Nominal and perturbed pole locations

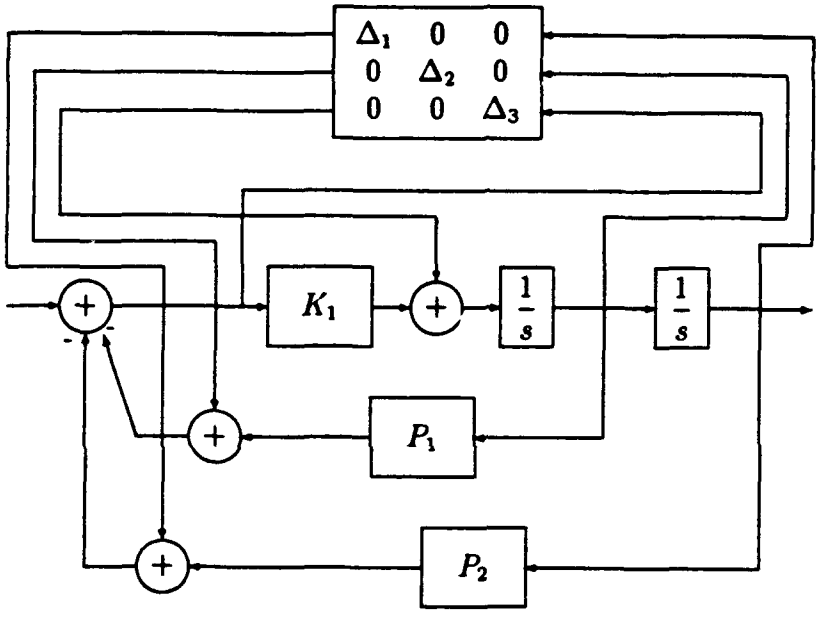

Figure 3.5: Block diagram for parametric uncertainties

magnitude with arbitrary phase. As an example, Figure 3.6 shows the nominal pole location along with variations in $P1$ with magnitude $\mid \Delta P1 \mid_{max}$ and phase varying from 0 to 2π. The pole motion describes a circle around the nominal pole location. (The circle is not perfect since the sensitivity changes with parameter variations as described above.)

We now consider variations in all three parameters simultaneously. For three perturbations, there will be eight (2^3) possible pole locations when evaluated at the scalar extremes. Figure 3.7 shows the nominal and perturbed pole locations. The maximum $\Delta\lambda$ occurs for the pole at $-11.8 \pm j2.4$. The parameters at this location are described by:

$$\begin{aligned} P1 &= P1_o + \Delta P1_{max} \\ P2 &= P2_o - \Delta P2_{max} \\ K1 &= K1_o + \Delta K1_{max} \end{aligned}$$

An H_∞ controller designed for these perturbations should then accommodate all variations within a radius of $\mid \Delta\lambda_{max} \mid$. In order to reduce the number of uncertainties used for H_∞ design, we observe that the variation in a single parameter may be increased until the magnitude of the eigenvalue change equals that of the extreme multiple parameter case. In the above example, $\mid \Delta\lambda \mid_{max} = 10.99$. Table 3.1 suggests that this change may be achieved with a 116% variation in $P1$, calculated as follows. The largest eigenvalue sensitivity is 69.3 at $P1_o + \Delta P1_{max}$. Using this to provide an initial value for $\Delta P1_{req}$:

$$\begin{aligned} \Delta p &= \frac{\mid \Delta\lambda \mid_{max}}{\Delta\lambda/\Delta p} \qquad (3.18) \\ \Delta P1_{req} &= \frac{\mid \Delta\lambda \mid_{max}}{\Delta\lambda/\Delta P1} = \frac{10.99}{69.3} = 0.1586 \\ \frac{\Delta P1}{P1} &= \frac{0.1586}{0.14} = 1.16 \end{aligned}$$

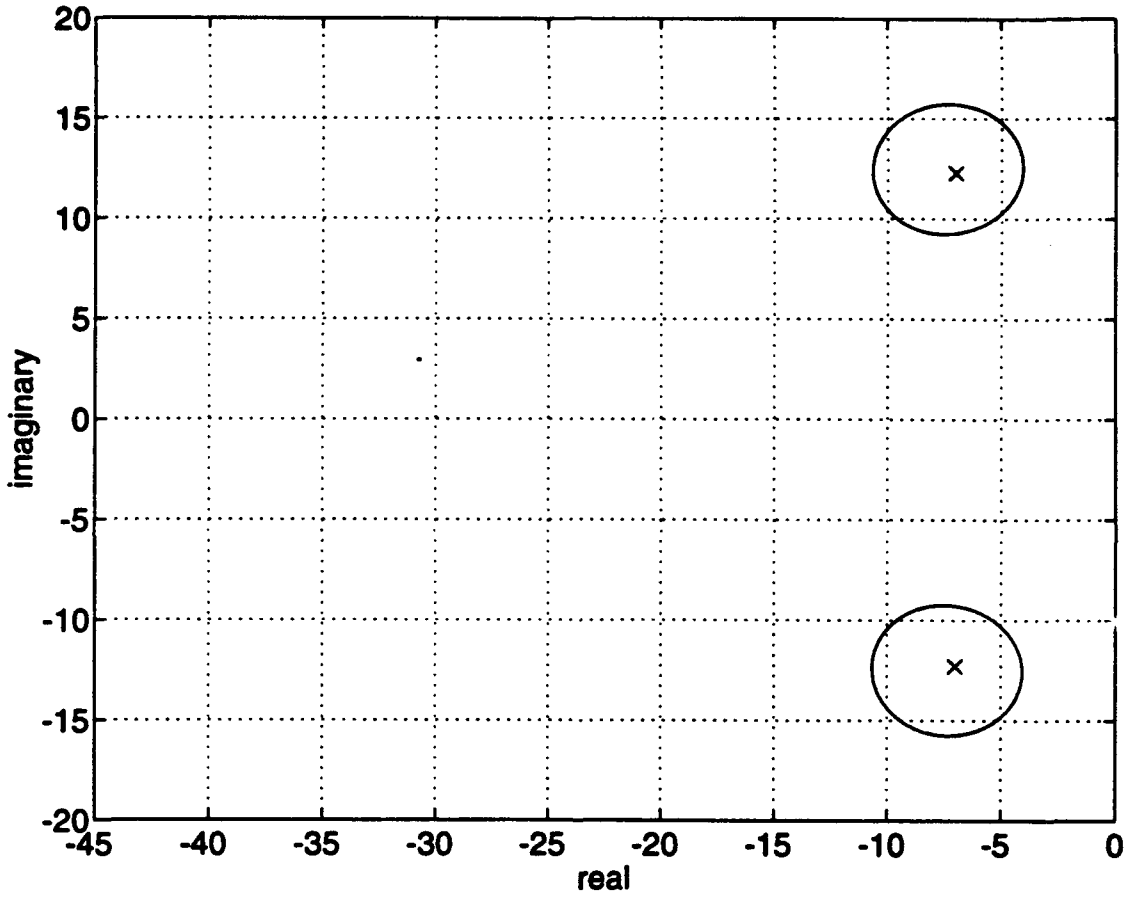

Figure 3.6: Pole locations for arbitrary phase locations

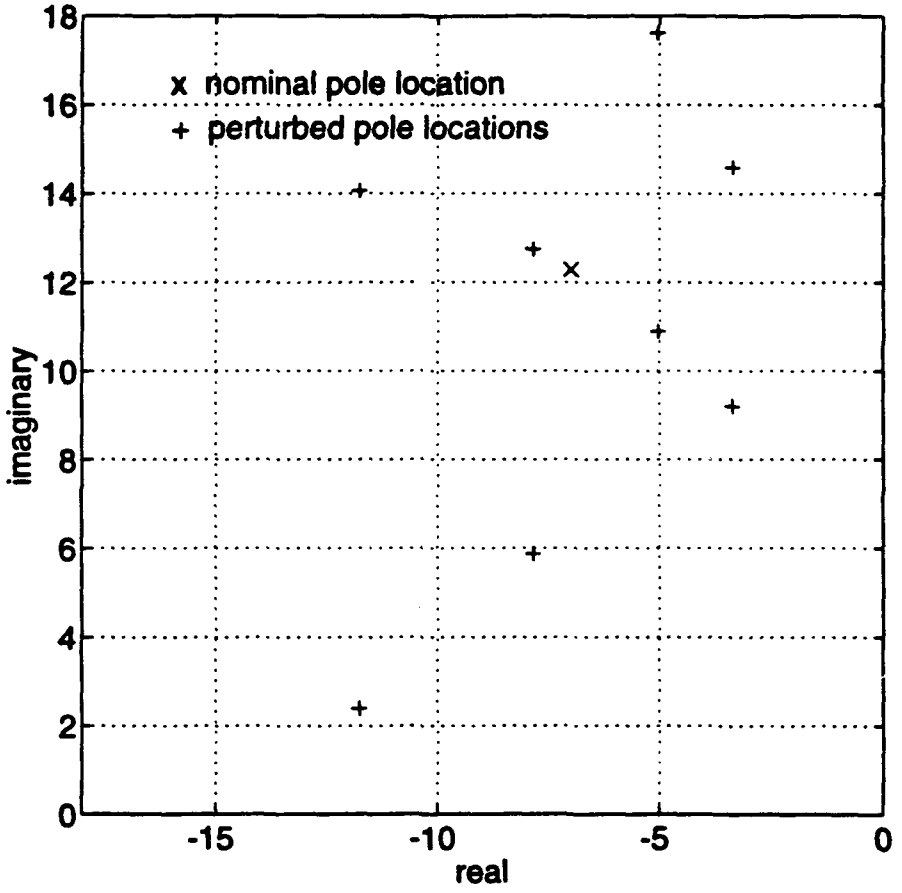

Figure 3.7: Nominal and Perturbed Pole Locations

Figure 3.8 shows the pole location associated with this variation. Note that 116% variation is greater than that required, as the complex poles have become real. (This is not unexpected since the pole sensitivity increases as $\Delta P1$ increases in the positive direction.) We iterate by taking successively smaller values of $\Delta P1$ and find that the required $\mid \Delta\lambda \mid_{max}$ is found to occur for a variation of 95.5% as shown in Figure 3.9. An H_∞ controller may now be designed using a variation of 95.5% in $P1$. Uncertainties of 40% in $P1$ and $P2$, and 20% in $K1$ should then be accommodated in the design.

The parametric uncertainty reduction process can be summarized as follows:

1. Calculate the eigenvalue sensitivity for each of the uncertain parameters at its nominal value.

2. Calculate the maximum eigenvalue change for each eigenvalue affected by the uncertain parameters.

3. Group parameters affecting the same eigenvalue and select one or more for scaling. (The examples in Chapter IV will provide some insight into this selection process.)

4. Calculate the eigenvalue sensitivity for the maximum parameter perturbations and scale the appropriate parameter uncertainties to accommodate the maximum eigenvalue change determined above.

5. Use the scaled uncertainties in the H_∞ design process in place of the original uncertainties.

6. If the resulting closed loop system is robust in the presence of the scaled uncertainties, verify the design by testing the controller with the system containing the original unscaled uncertainties.

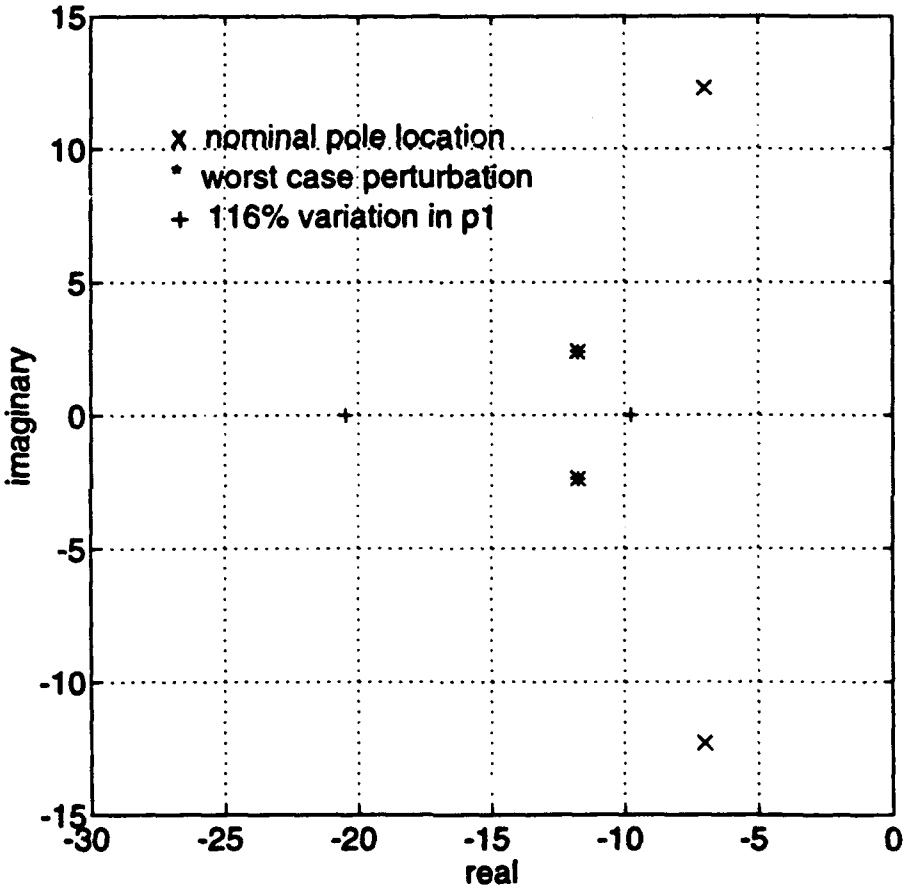

Figure 3.8: Pole location With 116% variation in p1

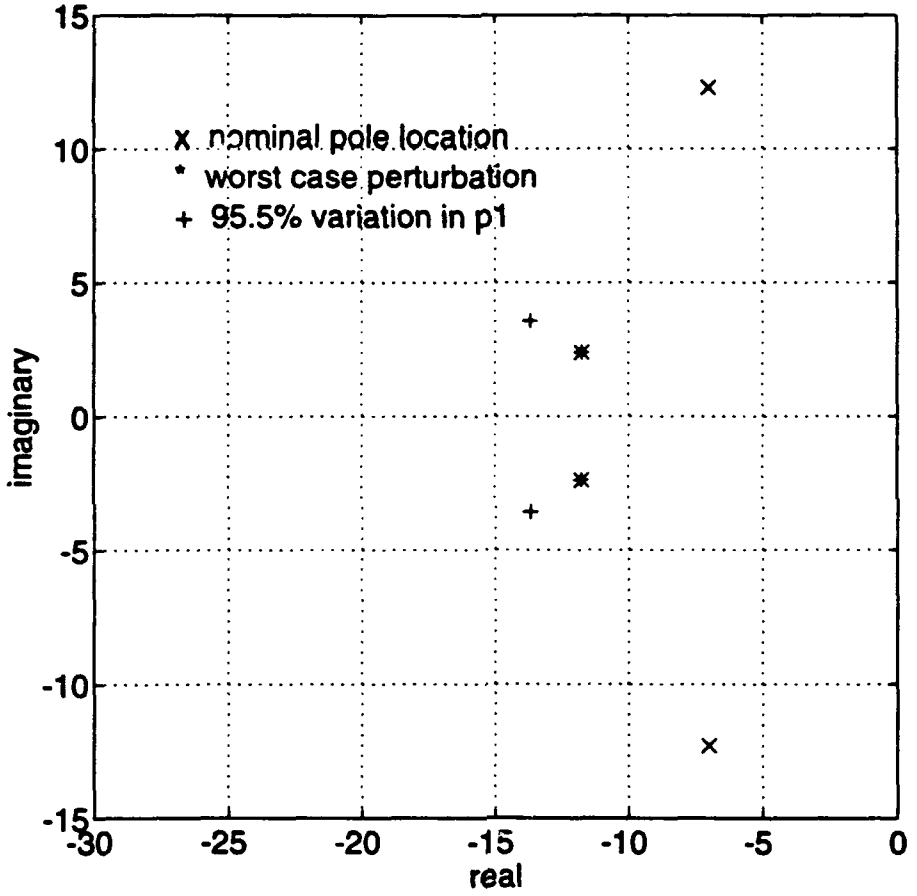

Figure 3.9: Pole location with 95.5% variation in p1

In Chapter IV, we use three examples to demonstrate the above uncertainty reduction technique in the design of a robust H_∞ controller.

IV. APPLICATIONS

A technique for reducing the number of parametric uncertainties needed for the design of a robust H_∞ controller was presented in Chapter III. In this chapter, that technique will be applied to three dynamic LTI systems. Parametric uncertainty reduction will first be used to design a robust H_∞ controller for a simple four state system with five uncertainties. Next, the procedure will be applied to the design of pitch plane autopilots for two different missile models.

A. GENERIC FOUR STATE MODEL

1. Model Description

An uncertain four state system is depicted in Figure 4.1. The system is similar to that used in the example in Chapter III with the addition of two more states and two uncertain parameters. The model has a single control input and feeds back one state and an error signal to the controller. The model in standard form appears in Figure 4.2. The plant has two exogenous inputs, the reference and a disturbance term. (The disturbance has been added to fulfill the constraint, mentioned in Chapter II, that D_{21} be of full rank.) The disturbance has a nominal weight of $W_{dist} = 0.001$. There are five uncertainties and two performance weights. The controller generates a single command input. All five parameters in the plant are assumed to be uncertain around a nominal value. Table 4.1 lists the nominal value for each parameter and its associated uncertainty.

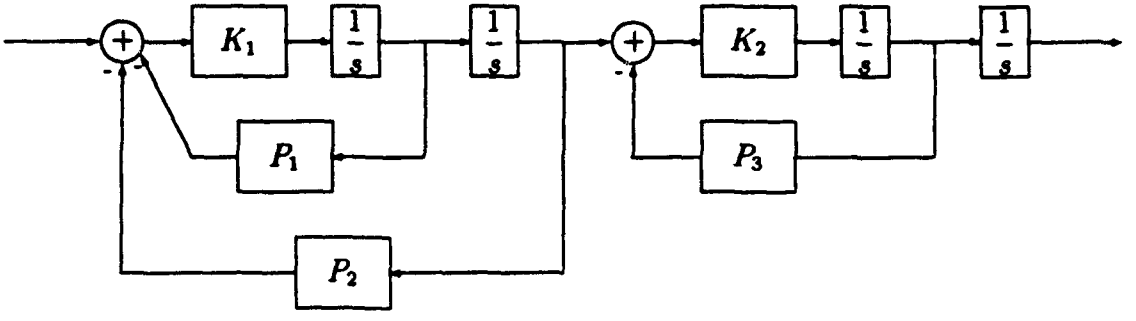

Figure 4.1: Four state system

TABLE 4.1: NOMINAL SYSTEM PARAMETERS AND UNCERTAINTIES

Parameter	Uncertainty
$P1_o = 0.14$	$\mid \Delta P1 \mid_{max} = 0.4 * P1_o$
$P2_o = 8$	$\mid \Delta P2 \mid_{max} = 0.4 * P2_o$
$P3_o = 2$	$\mid \Delta P2 \mid_{max} = 0.4 * P3_o$
$K1_o = 100$	$\mid \Delta K1 \mid_{max} = 0.2 * K1_o$
$K2_o = 4$	$\mid \Delta K2 \mid_{max} = 0.2 * K2_o$

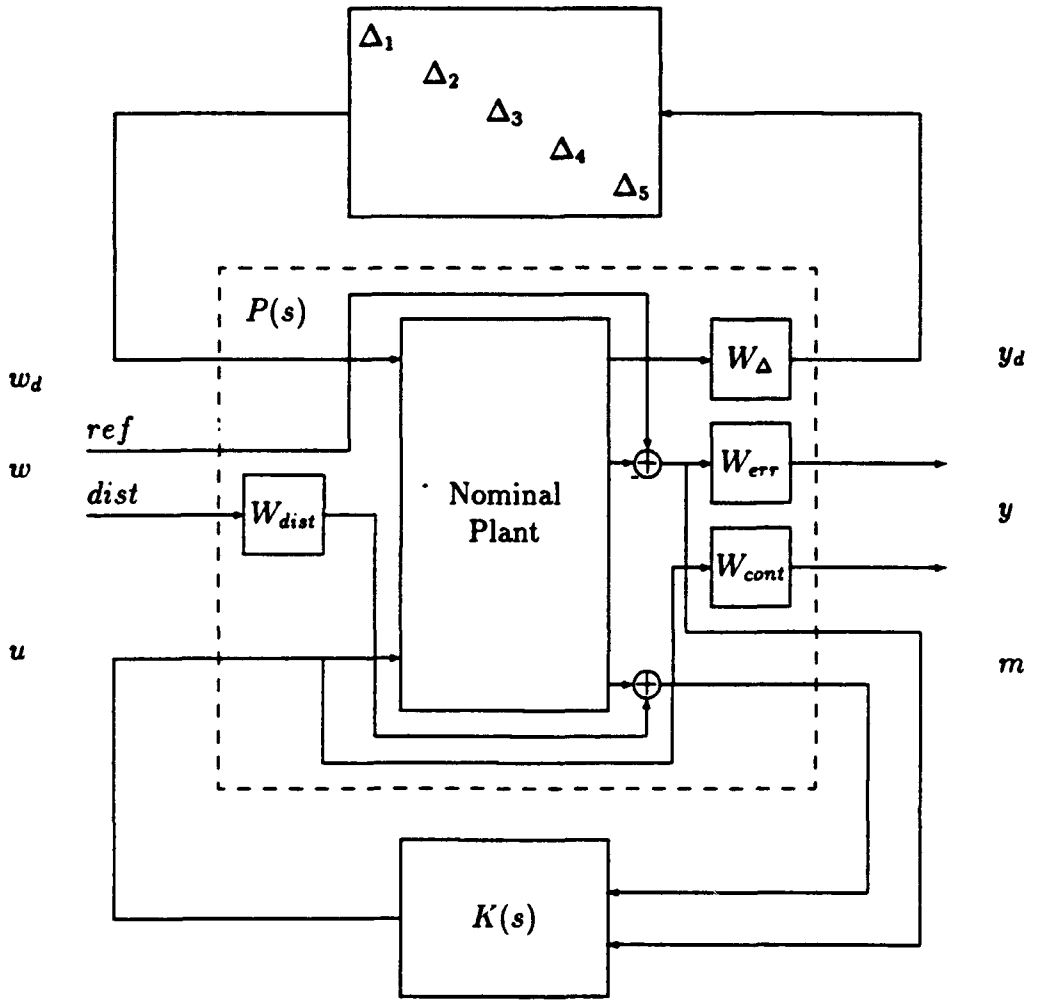

Figure 4.2: Four state system in standard form

a. Performance Weighting Functions

We define two performance weighting functions for the system, a weight on the error between the reference and the system output and a weight on the control input. The control weight, W_{cont}, is set arbitrarily small at 0.001. We include the weighted control as an output only to fulfill the constraint that the matrix term D_{12} be of full rank as mentioned in Chapter II. The error weighting function W_{err}, plotted in Figure 4.3, is a low pass filter with low frequency gain of 50, a gain crossover of 2 rad/sec and a high frequency gain of 0.125. This choice of weighting function should result in a steady-state error of less than 2%, closed loop time constant of 0.5 and minimal overshoot (Bibel and Malyevac, 1992). The transfer function of the error weight is

$$W_{err} = \frac{50(0.025s + 1)}{(10s + 1)} \tag{4.1}$$

The goal is to design an H_∞ controller which meets stability and robustness criteria taking into account all five uncertainties.

2. H_∞ Controller Design

We first attempt to design a controller by including all five uncertainties in the plant model. The H_∞ controller design procedure of Chapter II was used in an attempt to generate a robust controller. The mu plot in Figure 4.4 shows the SSV for robust performance and stability and the principle gains for nominal performance after three D-K iterations. It is clear that the closed loop plant does not exhibit nominal or robust performance. Further iterations yielded no improvement. We next apply the uncertainty reduction technique to the system and again attempt to design a robust controller, this time with a reduced number of uncertainties.

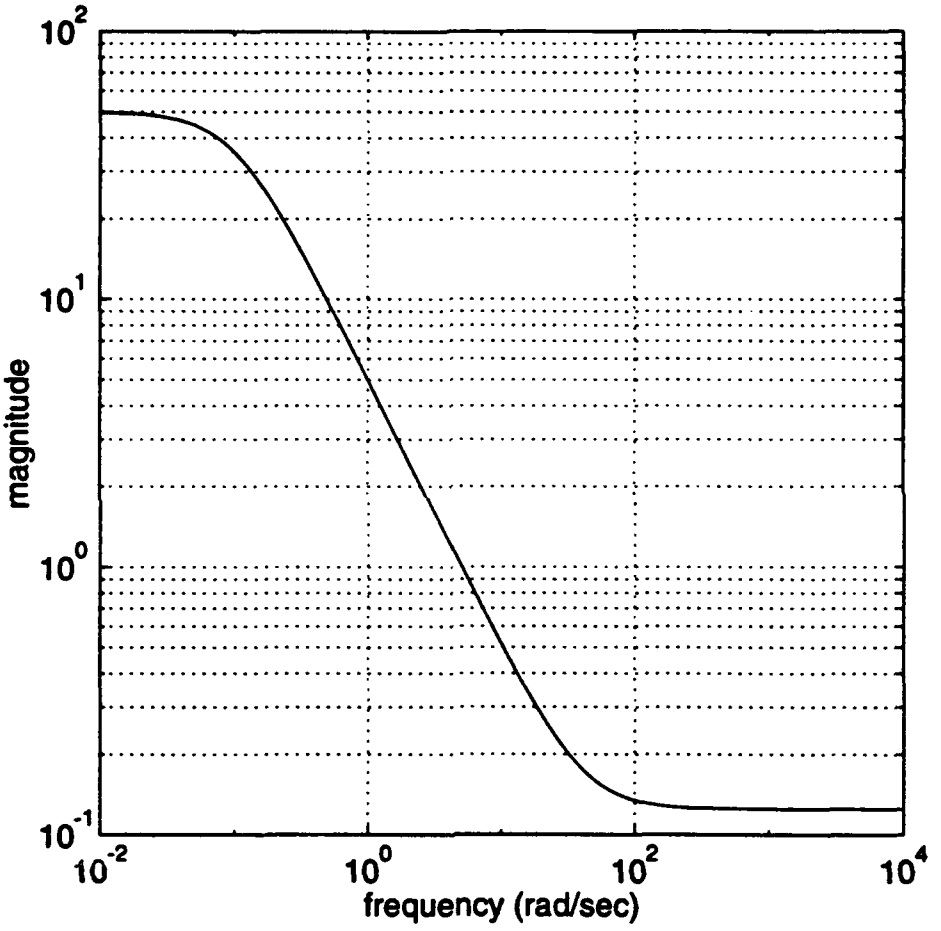

Figure 4.3: Reference error weighting function

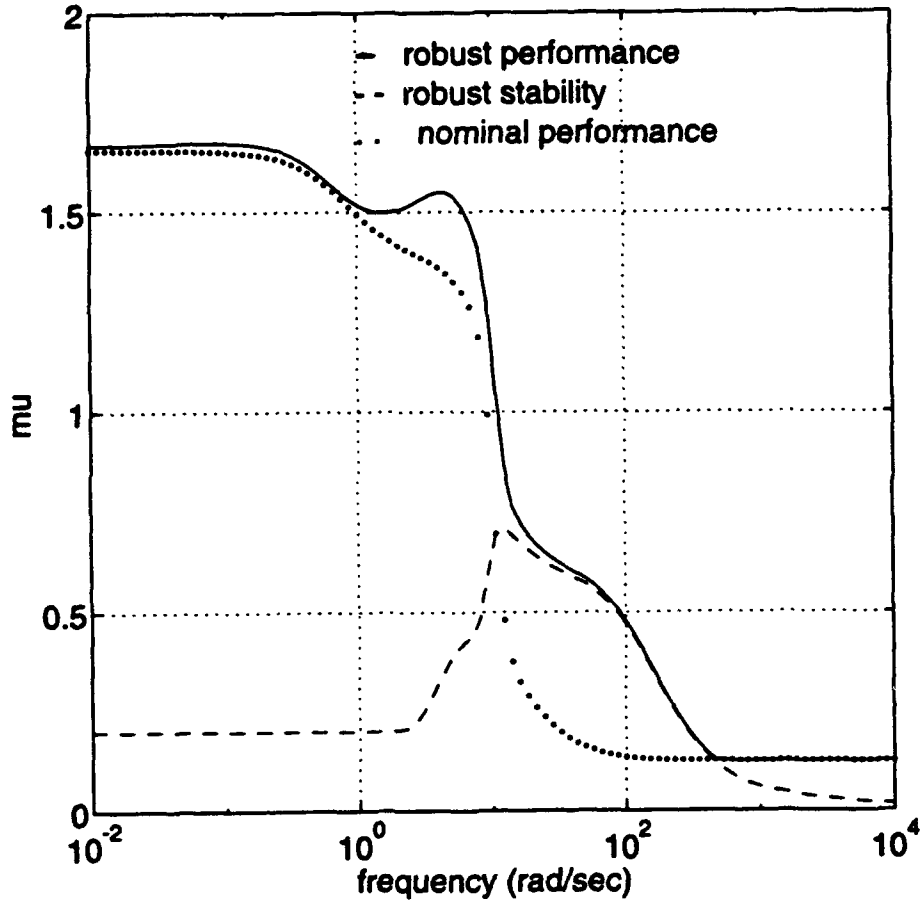

Figure 4.4: Robust analysis

3. Uncertainty Reduction

The eigenvalues of the nominal system are

$$\begin{aligned} \lambda_{1,2} &= -7 \pm j12.3; \\ \lambda_3 &= -32.0; \\ \lambda_4 &= 0. \end{aligned}$$

The eigenvalue sensitivity for all the plant parameters are shown in Table 4.2. We observe that $\lambda_{1,2}$ are affected only by parameters $P1, P2$, and $K1$, λ_3 by parameters $P3$ and $K2$, while the pole at the origin remains unaffected. The maximum eigenvalue changes for all combinations of parameter variations was found using the procedure in Chapter III to be

$$\begin{aligned} \mid \Delta\lambda_{1,2} \mid_{max} &= 10.99; \\ \mid \Delta\lambda_3 \mid_{max} &= 21.76. \end{aligned}$$

We select uncertainties $P1$ and $P3$ for scaling and apply Equation 3.18 to obtain an initial value for the scaled uncertainties:

$$\begin{aligned} \Delta P1 &= 1.16 * P1_o \\ \Delta P3 &= 0.68 * P3_o \end{aligned}$$

The eigenvalue sensitivity for $P3$ remains constant over the range of variation, and iteration, described in Chapter III, is not required. The eigenvalue sensitivity for parameter $P1$ varies, however, and we iterate to obtain the actual variation in $P1$ necessary to cause the required eigenvalue change,

$$\Delta P1_{req} = 0.955 * P1_o$$

TABLE 4.2: EIGENVALUE SENSITIVITY

			Eigenvalue Sensivitivy	
Eigenvalue	Parameter	Evaluated at	$\Delta\lambda/\Delta p$	$\lvert \Delta\lambda/\Delta p \rvert$
$-7 \pm j12.3$	$P1$	$P1_o$	$-50 \pm j28.5$	57.3
		$P1_o + \Delta P1_{max}$	$-50 \pm j48.1$	69.3
		$P1_o - \Delta P1_{max}$	$-50 \pm j15.6$	52.4
	$P2$	$P2_o$	$0 \mp j4.1$	4.1
		$P2_o + \Delta P2_{max}$	$0 \mp j3.3$	3.3
		$P2_o - \Delta P2_{max}$	$0 \mp j5.9$	5.9
	$K1$	$K1_o$	$-0.07 \mp j0.04$	0.080
		$K1_o + \Delta K1_{max}$	$-0.07 \mp j0.03$	0.076
		$K1_o - \Delta K1_{max}$	$-0.07 \mp j0.05$	0.088
	$P3$	$P3_o$	0	0
	$K2$	$K2_o$	0	0
-32.0	$P1$	$P1_o$	0	0
	$P2$	$P2_o$	0	0
	$K1$	$K1_o$	0	0
	$P3$	$P3_o$	$-4 + j0$	4
		$P3_o + \Delta P3_{max}$	$-4 + j0$	4
		$P3_o - \Delta P3_{max}$	$-4 + j0$	4
	$K2$	$K2_o$	$-8 + j0$	8
		$K2_o + \Delta K2_{max}$	$-8 + j0$	8
		$K2_o - \Delta K2_{max}$	$-8 + j0$	8
0	$P1$	$P1_o$	0	0
	$P2$	$P2_o$	0	0
	$K1$	$K1_o$	0	0
	$P3$	$P3_o$	0	0
	$K2$	$K2_o$	0	0

4. Controller Design for Reduced Uncertainties

Using only the scaled uncertainties in $P1$ and $P3$, it was possible to design an H_∞ controller exhibiting desired robustness properties in the presence of the scaled uncertainties. The mu plot in Figure 4.5 displays the SSV for robust performance and stability, and the principle gains for nominal stability. All plots remain below one, indicating a robust design. Our interest, however, is in the original plant with five uncertainties. Using the controller designed for the scaled uncertainty plant, robust analysis of the complete plant resulted in the mu plot of Figure 4.6. It is clear that the system meets robust stability and nominal and robust performance specifications.

We next examine the time response of the final closed loop system to verify that performance objectives are met. Figure 4.9, showing the system response to a unit step input, reveals a rise time of 0.23 seconds, a maximum overshoot of 4.4% and a steady state error of 1.73%. This confirms that the performance goals of minimal overshoot and less than 2% steady-state error are satisfied.

5. Controller Design Ignoring Some Uncertainties

It is interesting to investigate the effect of controller design ignoring several of the uncertainties in the system. We may be tempted to use this approach when the inclusion of all uncertainties results in a failure to design a robust controller, as in subsection 2. Considering only the 40% uncertainties in $P1$ and $P3$, and ignoring uncertainties in $P2$, $K1$ and $K2$, an H_∞ controller was designed. When tested against the plant with all five uncertainties, however, the SSV exceeds one as shown in Figure 4.8, implying that the robust performance objective is not met. It is clear that simply ignoring uncertainties may often result in a closed loop plant which lacks robustness.

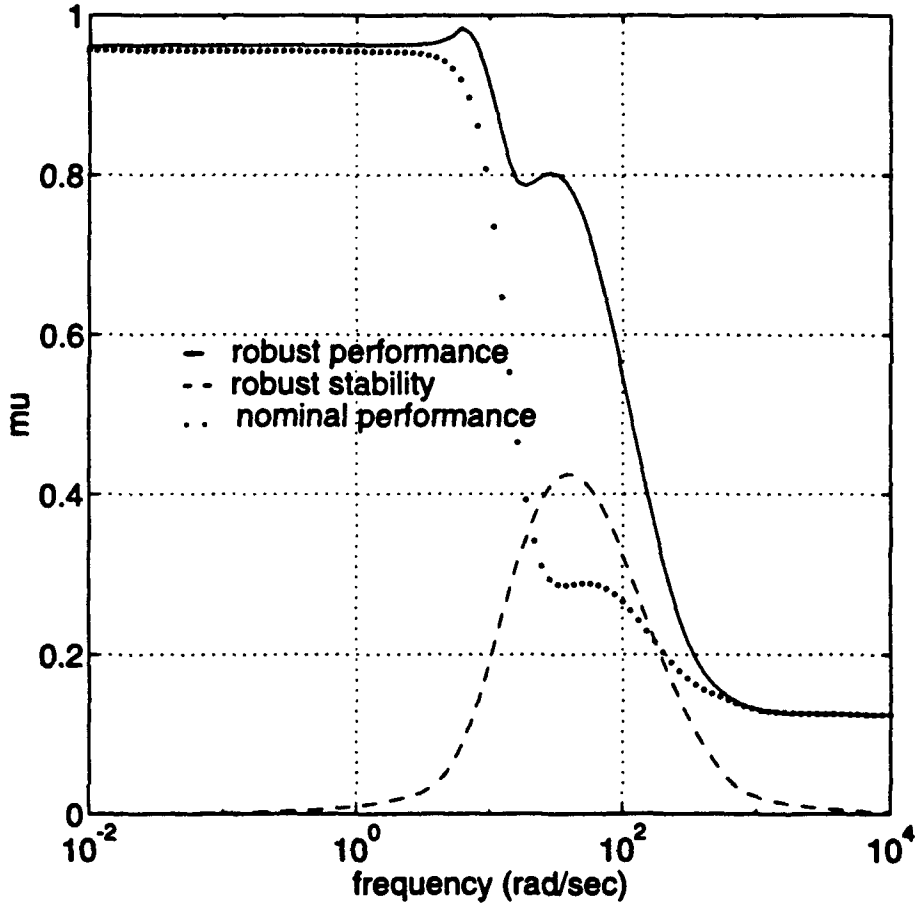

Figure 4.5: Robust analysis for scaled uncertainty plant

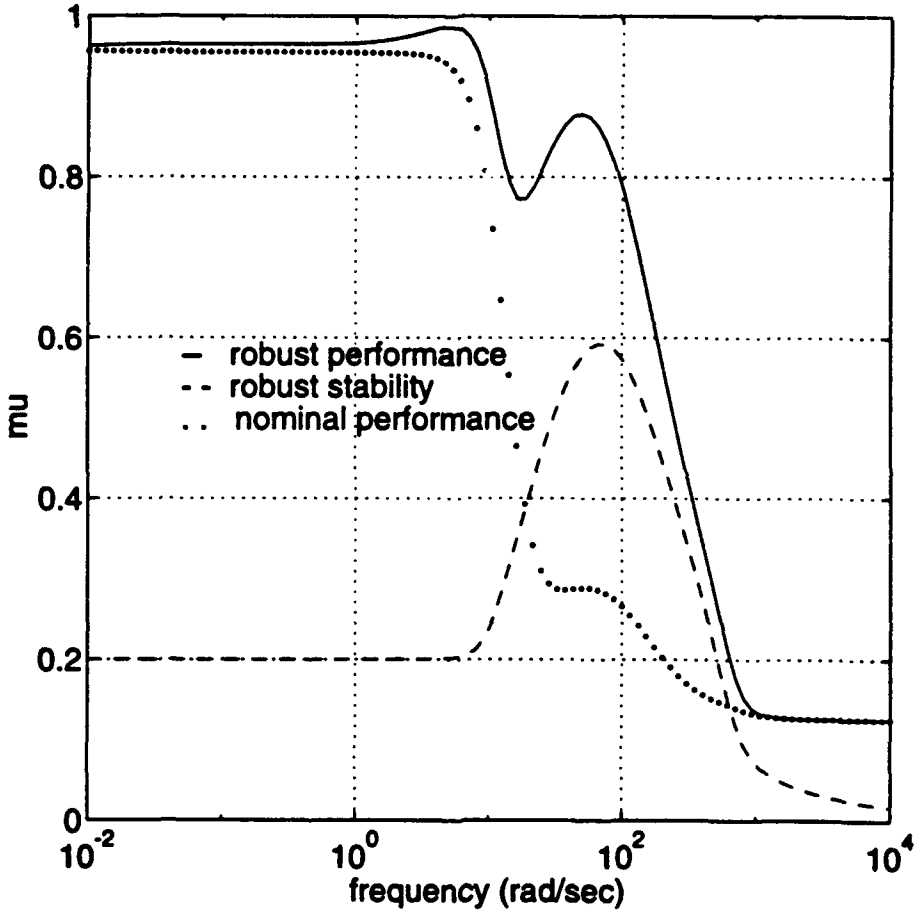

Figure 4.6: Robust analysis for plant with all uncertainties

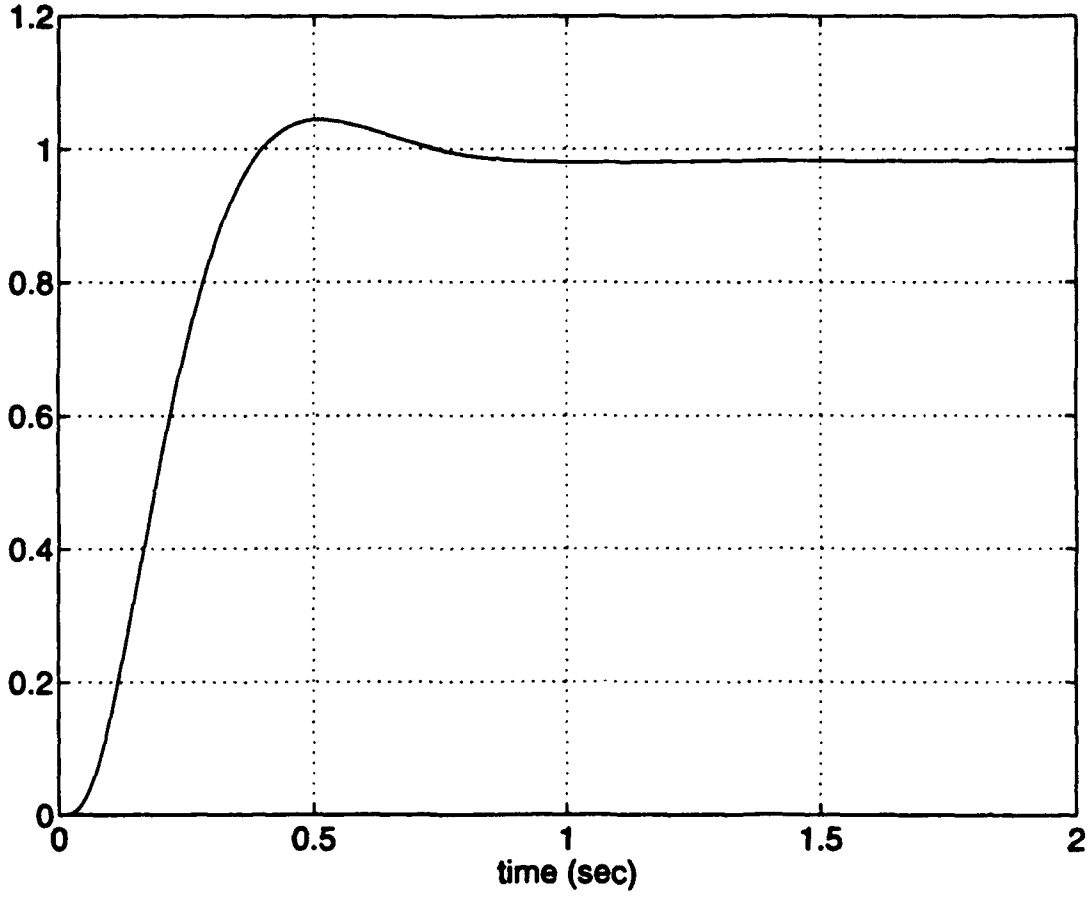

Figure 4.7: Step response

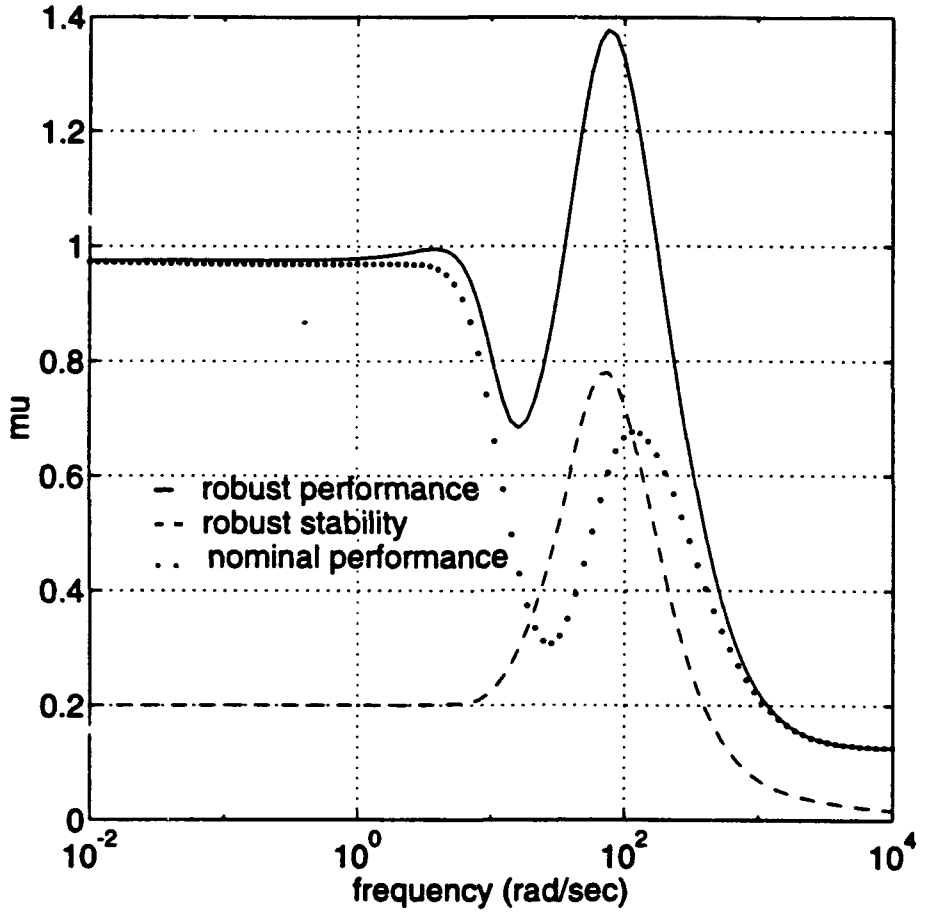

Figure 4.8: Robust analysis for plant ignoring some uncertainties

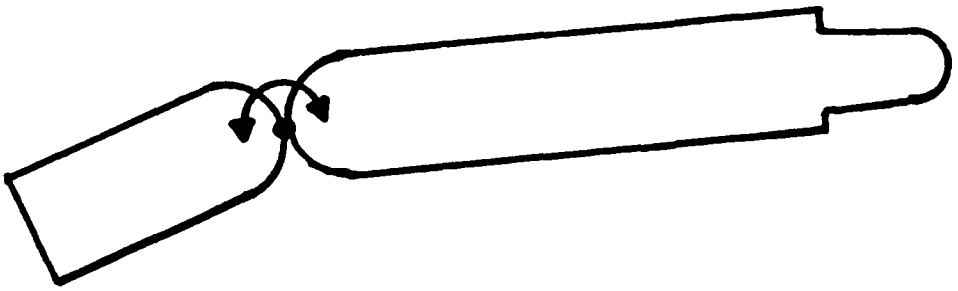

Figure 4.9: Low-drag ramjet model

B. COMBUSTOR CONTROLLED MISSILE

We next apply the uncertainty reduction technique to a pitch plane autopilot for a low-drag ramjet missile model. This model, shown in Figure 4.9, is controlled by a moveable combustor section and has no external control surfaces on the missile. The model has five uncertain parameters affecting two real poles and a set of complex poles. The linearized model of this missile was developed by the Naval Air Warfare Center, China Lake, CA (Robins, 1992).

1. Missile Model

The block diagram of the missile is shown in Figure 4.10. The input to the system is a commanded combustor deflection angle, δ_c in radians. The outputs of the system are missile acceleration η, and pitch rate q. The missile model was linearized at one operating altitude and velocity. The varying factors affecting the plant are angle of attack and missile mass. Seven parameters are affected by these changes, H_α, H_δ, Z_α, Z_δ, M_α, M_δ and I_b. Of these, H_α and H_δ do not affect the eigenvalues. Table 4.3 lists the nominal value for each parameter along with uncertainties in the

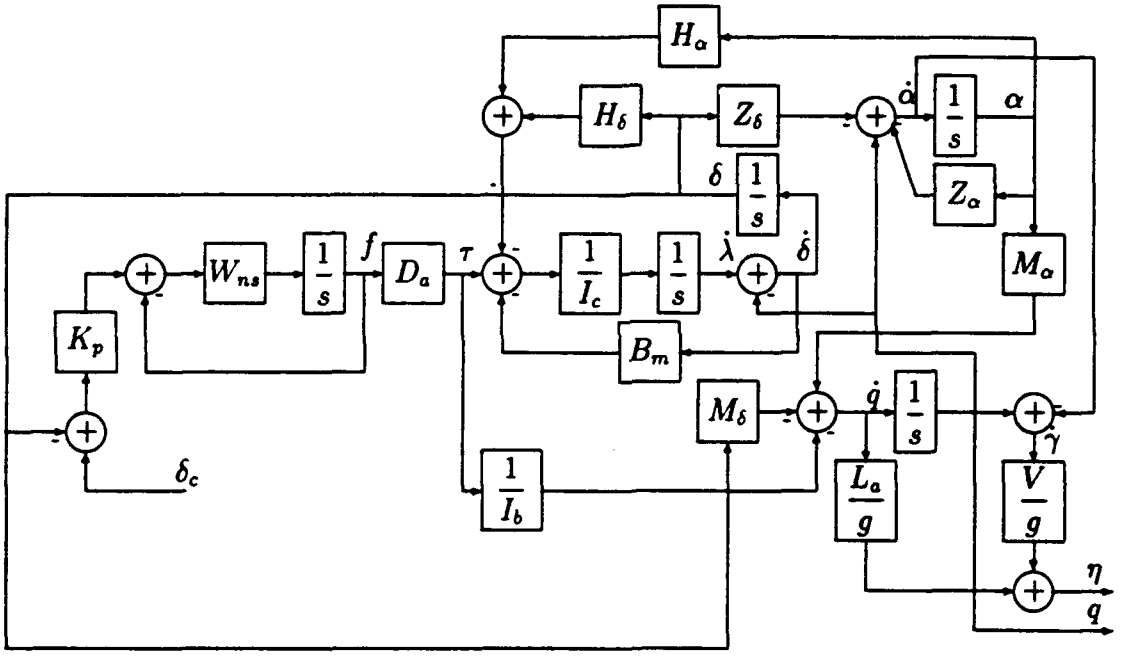

Figure 4.10: Low-drag ramjet block diagram

TABLE 4.3: NOMINAL SYSTEM PARAMETERS AND UNCERTAINTIES

Parameter	Uncertainty
$I_{b_o} = 201$	$\mid \Delta I_b \mid_{max} = 0.21 * I_{b_o}$
$M_{\alpha_o} = 760.79$	$\mid \Delta M_\alpha \mid_{max} = 0.24 * M_{\alpha_o}$
$M_{\delta_o} = 341.59$	$\mid \Delta M_\delta \mid_{max} = 0.51 * M_{\delta_o}$
$Z_{\alpha_o} = 0.5099$	$\mid \Delta Z_\alpha \mid_{max} = 0.34 * Z_{\alpha_o}$
$Z_{\delta_o} = 0.2165$	$\mid \Delta Z_\delta \mid_{max} = 0.41 * Z_{\delta_o}$
$Kp = 65,000$	
$W_{ns} = 225$	
$Da = 1.17$	
$H_\alpha = 10,324$	
$H_\alpha = 11,595$	
$Ic = 14.5$	
$La/g = 0.1739$	
$V/g = 107.2981$	
$Bm = 1523$	

varying parameters listed above.

a. Performance Weighting Functions

For this system we define two performance weighting functions, one weighting the error between the reference input and output acceleration and one weighting the combustor deflection angle. The error weight is a low pass filter shown in Figure 4.11. It has a DC gain of 50, corresponding to a 2% steady-state error. The combustor deflection weight is set equal to the inverse of the maximum allowable deflection of 10 degrees.

2. H_∞ Controller Design

An attempt was made to design a robust H_∞ controller including all five uncertainties in the plant. The SSV plot of Figure 4.12 reveals that the process failed to produce a controller exhibiting robust performance. We next apply the parametric uncertainty reduction technique and again attempt to design a robust controller.

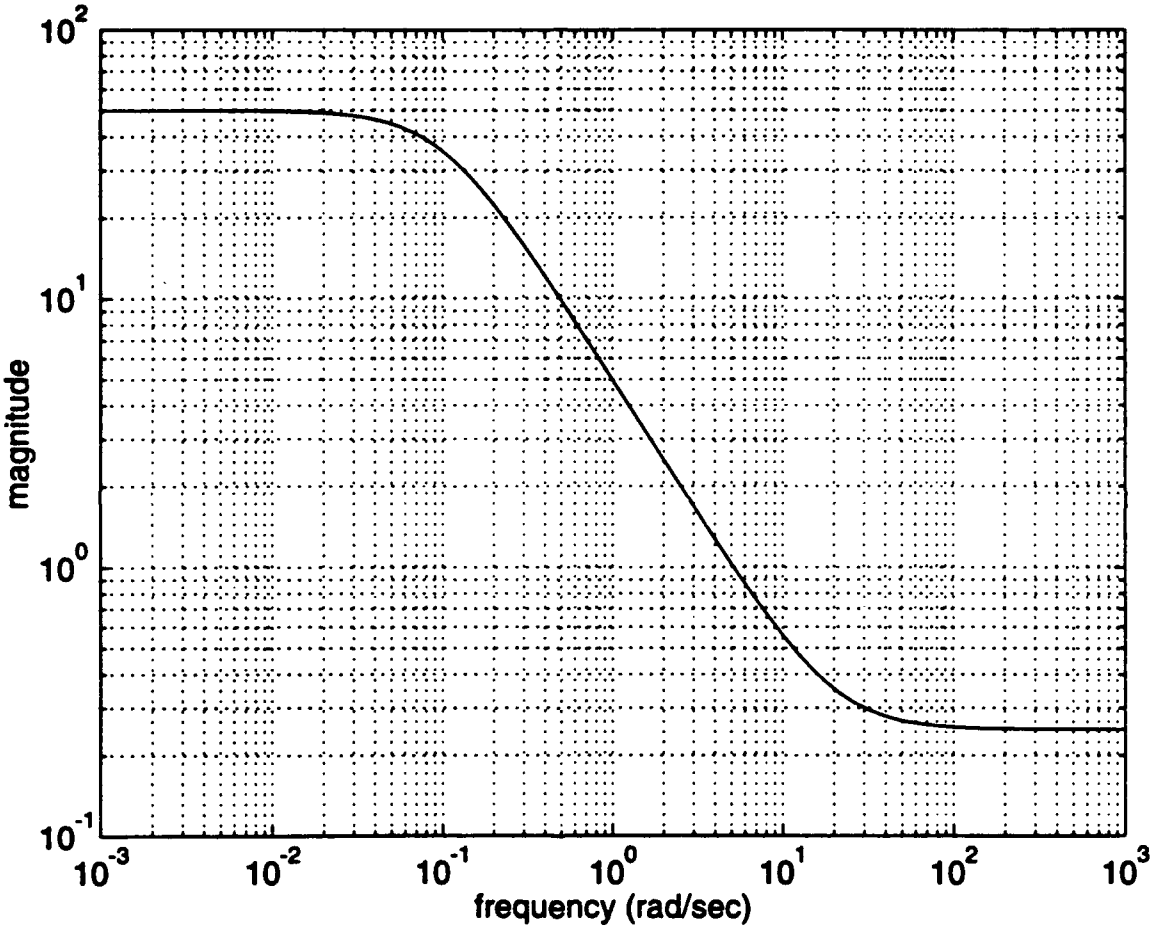

Figure 4.11: Reference error weighting function

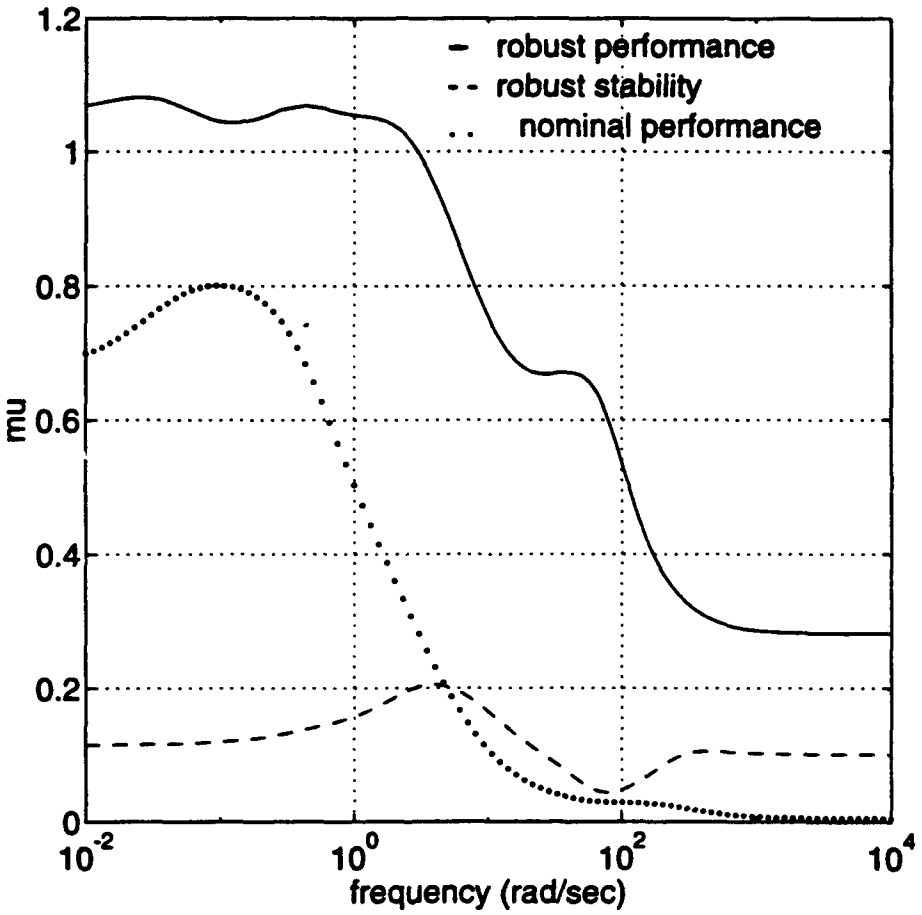

Figure 4.12: Robust analysis

3. Uncertainty Reduction

The eigenvalues of the nominal system are

$$\begin{aligned} \lambda_{1,2} &= -36.76 \pm j62.7 \\ \lambda_3 &= 27.35 \\ \lambda_4 &= -27.27 \\ \lambda_5 &= -257.11 \end{aligned}$$

and their eigenvalue sensitivities are listed in Table 4.4. Eigenvalue λ_5 is not affected by any of the varying parameters and has not been included. Following the procedures in Chapter III, the maximum eigenvalue changes for all possible combinations of parameter variations was found to be

$$\begin{aligned} |\,\Delta\lambda_{1,2}\,|_{max} &= 1.63 \\ |\,\Delta\lambda_3\,|_{max} &= 4.47 \\ |\,\Delta\lambda_4\,|_{max} &= 5.10 \end{aligned}$$

We select the parameters for scaling by examining Table 4.4. Parameter $1/I_b$, although affecting all four eigenvalues with large sensitivities, is sufficiently small that a variation of almost 200% would be required to accommodate the change in λ_3. Likewise, parameters Z_α and Z_δ have relatively small nominal values and sensitivities. We therefore choose to scale M_δ to satisfy the change in $\lambda_{1,2}$ and M_α for the change in λ_3 and λ_4. The initial scaling values are found as follows:

$$\Delta M_\delta = \frac{|\,\Delta\lambda_{1,2}\,|_{max}}{\Delta\lambda_{1,2}/\Delta M_\delta} = \frac{1.63}{0.006} = 271.67$$

$$\frac{\Delta M_\delta}{M_\delta} = \frac{271.67}{341.59} = 0.79$$

TABLE 4.4: EIGENVALUE SENSITIVITY

			Eigenvalue Sensivitivy	
Eigenvalue	Parameter	Evaluated at	$\Delta\lambda/\Delta p$	$\lvert \Delta\lambda/\Delta p \rvert$
$-36.7 \pm j62.7$	$1/I_b$	I_{b_o}	$14.2 \mp j514$	515.1
	Z_δ	Z_{δ_o}	$0.13 \mp j0.05$	0.14
	Z_α	Z_{α_o}	0	0
	M_α	M_{α_o}	$-1.6e^{-4} \mp j3.1e^{-5}$	$1.68e^{-4}$
		$M_{\alpha_o} + \Delta M_{\alpha_{max}}$	$-1.6e^{-4} \mp j2.3e^{-5}$	$1.62e^{-4}$
		$M_{\alpha_o} - \Delta M_{\alpha_{max}}$	$-1.6e^{-4} \mp j4.5e^{-5}$	$1.75e^{-4}$
	M_δ	M_{δ_o}	$0.0017 \pm j0.006$	0.006
		$M_{\delta_o} + \Delta M_{\delta_{max}}$	$0.001 \pm j0.006$	0.006
		$M_{\delta_o} - \Delta M_{\delta_{max}}$	$0.002 \pm j0.006$	0.006
27.35	$1/I_b$	I_{b_o}	-213.88	213.88
	Z_δ	Z_{δ_o}	0.09	0.09
	Z_α	Z_{α_o}	-0.5	0.5
	M_α	M_{α_o}	0.02	0.02
		$M_{\alpha_o} + \Delta M_{\alpha_{max}}$	0.016	0.016
		$M_{\alpha_o} - \Delta M_{\alpha_{max}}$	0.021	0.021
	M_δ	M_{δ_o}	0.003	0.003
		$M_{\delta_o} + \Delta M_{\delta_{max}}$	0.003	0.003
		$M_{\delta_o} - \Delta M_{\delta_{max}}$	0.003	0.003
-27.27	$1/I_b$	I_{b_o}	518.38	518.38
	Z_δ	Z_{δ_o}	0.17	0.17
	Z_α	Z_{α_o}	-0.5	0.5
	M_α	M_{α_o}	-0.020	0.020
		$M_{\alpha_o} + \Delta M_{\alpha_{max}}$	-0.016	0.016
		$M_{\alpha_o} - \Delta M_{\alpha_{max}}$	-0.021	0.021
	M_δ	M_{δ_o}	-0.006	0.006
		$M_{\delta_o} + \Delta M_{\delta_{max}}$	-0.006	0.006
		$M_{\delta_o} - \Delta M_{\delta_{max}}$	-0.006	0.006

$$\Delta M_\alpha = \frac{|\,\Delta\lambda_3\,|_{max}}{\Delta\lambda_3/\Delta M_\alpha} = \frac{4.47}{0.021} = 212.9$$

$$\frac{\Delta M_\alpha}{M_\alpha} = \frac{212.9}{760.79} = 0.28$$

$$\Delta M_\alpha = \frac{|\,\Delta\lambda_4\,|_{max}}{\Delta\lambda_4/\Delta M_\alpha} = \frac{5.10}{0.021} = 242.9$$

$$\frac{\Delta M_\alpha}{M_\alpha} = \frac{242.9}{760.79} = 0.32$$

By iterating, the required scaled uncertainties are found to be 80% in M_δ and 34% in M_α. These scaled uncertainties are next used to design a robust H_∞ controller.

4. Controller Design for Reduced Uncertainties

Using only the scaled uncertainties in parameters M_δ and M_α, a robust H_∞ controller has been designed. The plot of the SSV is shown in Figure 4.13. The design exhibits nominal performance and robust performance and stability in the presence of the two scaled uncertainties. The controller when tested against the plant with all five uncertainties yields the plot in Figure 4.14. The system again exhibits nominal and robust performance and robust stability.

The time response of the final closed loop system was analyzed to verify that performance criteria were met. The step response of the system, shown in Figure 4.15, shows an overdamped system with a rise time of 0.35 seconds and no overshoot. Steady state error was determined to be 0.5%. The initial transient spike is a result of the torque caused by the movement of the combustor section.

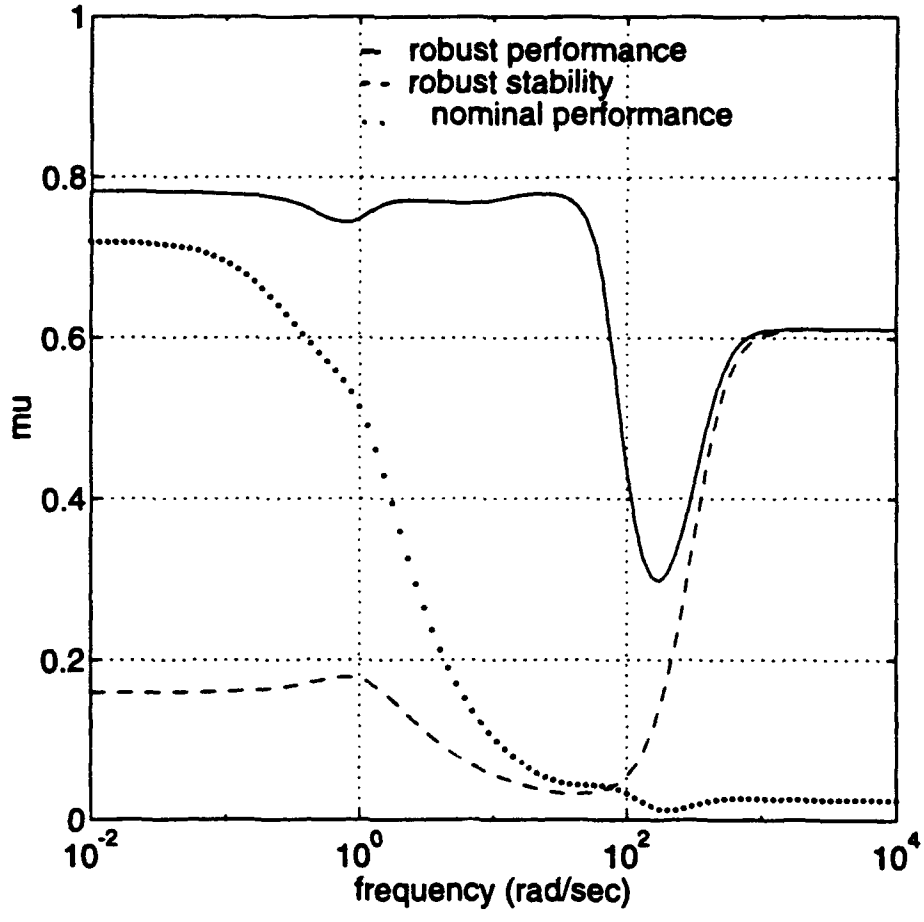

Figure 4.13: Robust analysis for scaled uncertainty plant

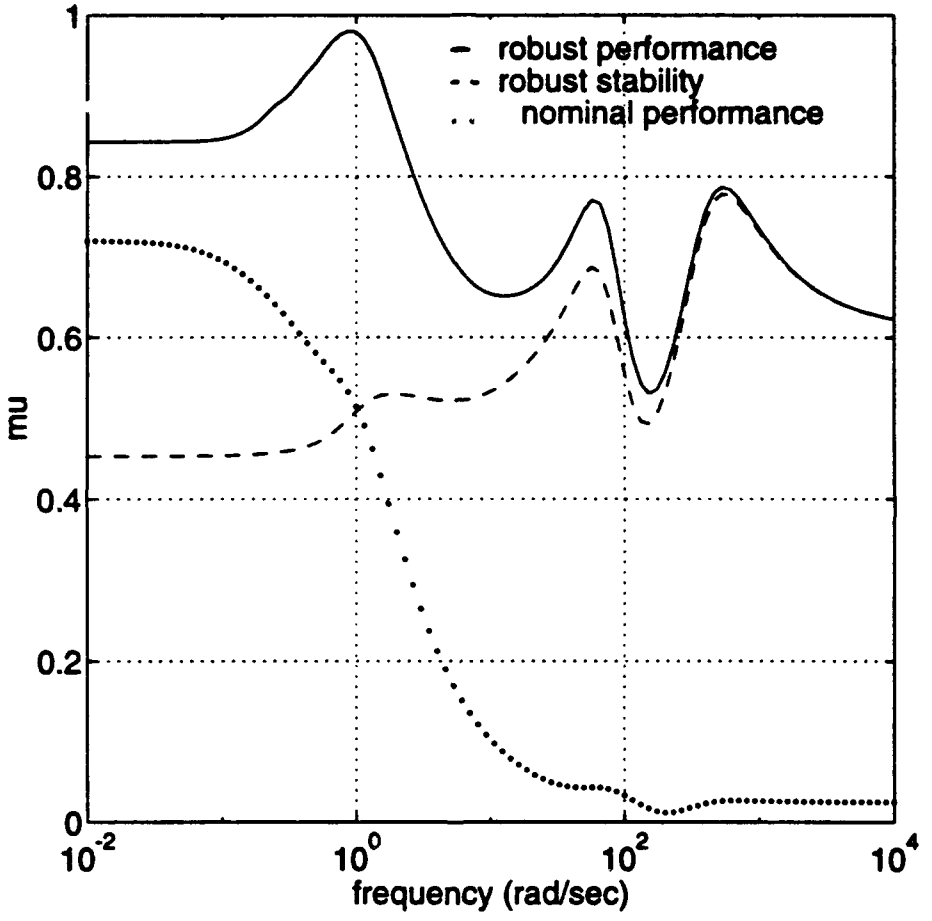

Figure 4.14: Robust analysis for plant with all uncertainties

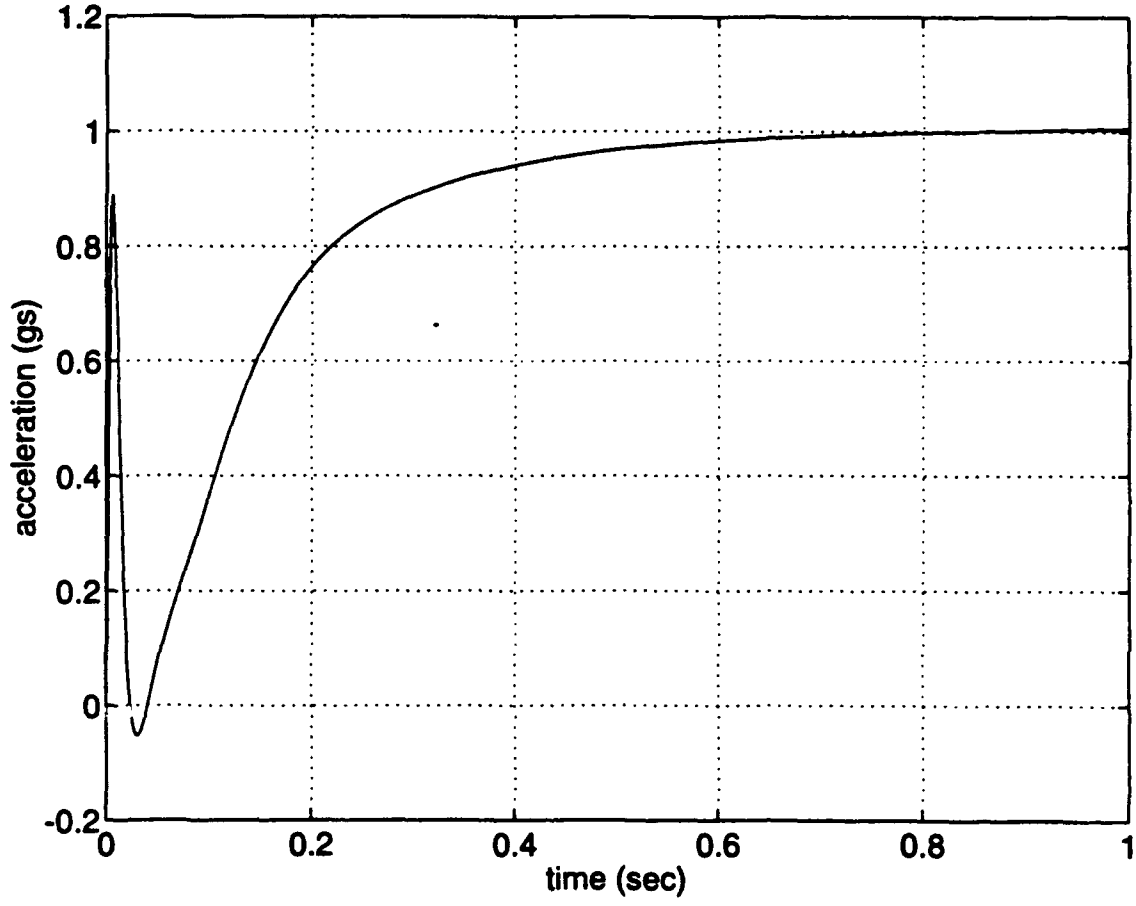

Figure 4.15: Step response

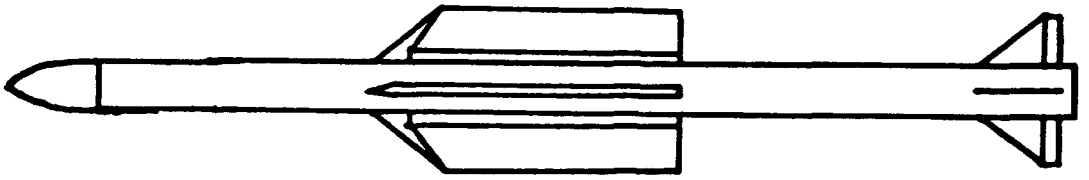

Figure 4.16: Tail fin controlled missile

C. TAIL FIN CONTROLLED MISSILE

The parametric uncertainty reduction technique is next applied to the pitch plane autopilot of a conventional tail fin controlled missile. The missile is depicted in Figure 4.16. This model has three uncertain parameters affecting one set of complex eigenvalues. One of the parameters varies 270%, however, causing the eigenvalues to shift from complex to real over the range of uncertainty. A linearized model from the Naval Surface Warfare Center, Dahlgren, VA was used for analysis (Bibel and Stalford, 1991).

1. Missile Model

The block diagram of the missile is shown in Figure 4.18. The input to the system is a commanded tail fin deflection angle, δ_c. The system outputs are missile acceleration, η, and pitch rate, q, from the accelerometer and gyro, respectively.

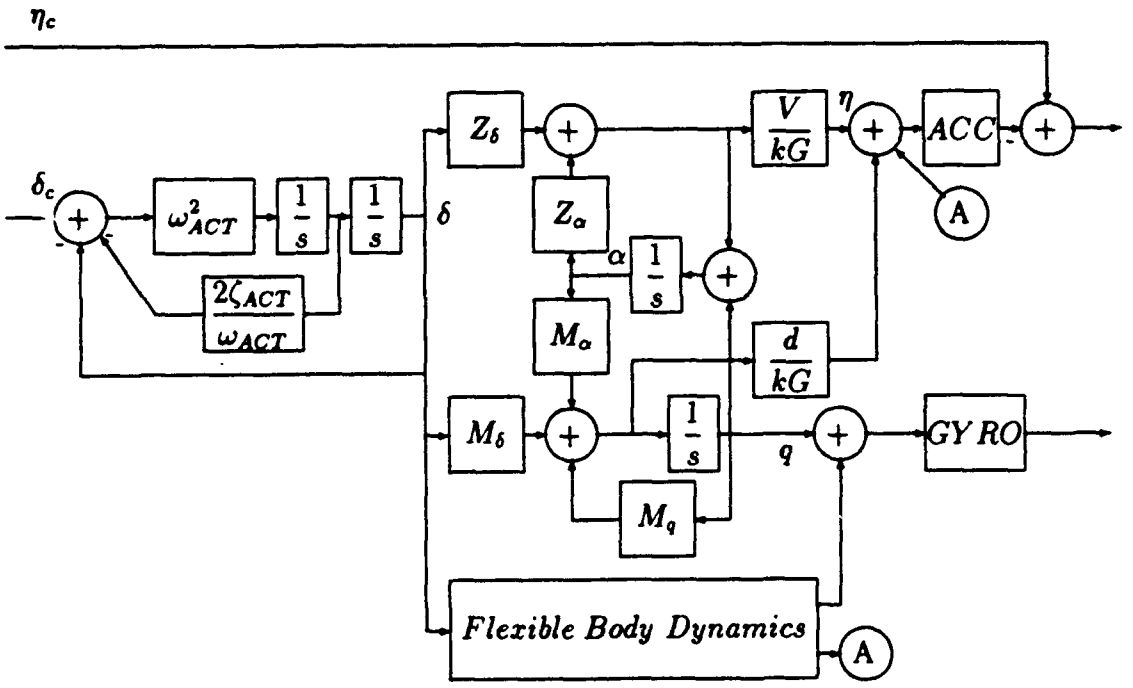

Figure 4.17: Conventional missile block diagram

TABLE 4.5: NOMINAL PARAMETERS AND UNCERTAINTIES

Parameter	Uncertainty
$Z_{\alpha_o} = -5.24$	$\mid \Delta Z_{\alpha_{max}} = 2.72 * Z_{\alpha_o}$
$M_{\alpha_o} = -46.97$	$\mid \Delta M_{\alpha_{max}} = 0.15 * M_{\alpha_o}$
$M_{q_o} = -4.69$	$\mid \Delta M_{q_{max}} = 0.3 * M_{q_o}$
$Z_\delta = -0.73$	
$M_\delta = -1134$	
$d/kG = 8.55e^{-4}$	
$V/kG = 1.8154$	

TABLE 4.6: FLEXIBLE BODY MODE PARAMETERS

ω_n	K_{qn}	K_{η_n}
368.0	1204.1	-0.943
937.0	406.5	0.561
1924.0	-1408.4	-0.312

a. Nominal System Parameters and Uncertainties

The linear model has been developed for one particular altitude and velocity. Factors affecting the plant parameters are angle of attack, α, and pitch rate, q which cause changes in the parameters M_α, Z_α and M_q. The nominal parameters and associated uncertainties are listed in Table 4.5. The actuator is modeled as a second order transfer function with a damping of $\zeta_{ACT} = 0.7$ and a natural frequency of $\omega_{ACT} = 188.5$ rad/sec. The actuator has a fin deflection limit of 40 degrees and a fin rate limit of 300 degrees/sec. The input to the actuator is the command input, δ_c. The model includes flexible bending modes which are modeled as second order transfer functions. The first three bending modes have been included, and the nth mode effect on acceleration and pitch rate is given by

$$\begin{bmatrix} q(s) \\ \eta(s) \end{bmatrix}_{fb} = \frac{1}{s^2 + 2\zeta_{fb}\omega_n s + \omega_n^2} \begin{bmatrix} sK_{q_n} \\ s^2 K_{\eta_n} \end{bmatrix} \delta(s)$$

The data for the flexible modes is shown in Table 4.6. The controller acts on an accelerometer and pitch rate gyro, both modeled as second order devices with a

damping of 0.7 and natural frequencies $\omega_{ACC} = 377$ rad/sec and $\omega_{GYRO} = 500$ rad/sec. The model includes an input feedback uncertainty with a constant value of 0.2, and a second order input multiplicative uncertainty with a transfer function given by

$$W_{inp} = \frac{(1/100)(0.049s + 1)^2}{(9.805e^{-4}s + 1)^2}$$

b. Performance Weighting Functions

For this plant we define four performance weighting functions. Two of these are weights on the fin deflection and fin rate, set equal to the inverse of the allowable values of 40 degrees and 300 degrees/second, respectively. The performance weight on the error between the reference input and output acceleration is a first order transfer function described by

$$W_{err} = \frac{100(0.0258s + 1)}{10.327s + 1)} \tag{4.2}$$

The fourth performance function is a weight on the pitch rate. It is a high pass transfer function designed to attenuate the effects of unmodeled high frequency dynamics and sensor noise. It is described by

$$W_q = \frac{(1/400)(0.025s + 1)^2}{(1.78e^{-4}s + 1)^2} \tag{4.3}$$

The goal is to design a robust H_∞ controller taking into account all the uncertainties and performance weights.

2. H_∞ Controller Design

An attempt was made to design a robust H_∞ controller for the plant with all three uncertainties. Figure 4.18 shows the robust analysis results after four D-K iterations. The closed loop system does not possess robust or nominal performance. Uncertainty reduction techniques are next applied to the model in an effort to obtain

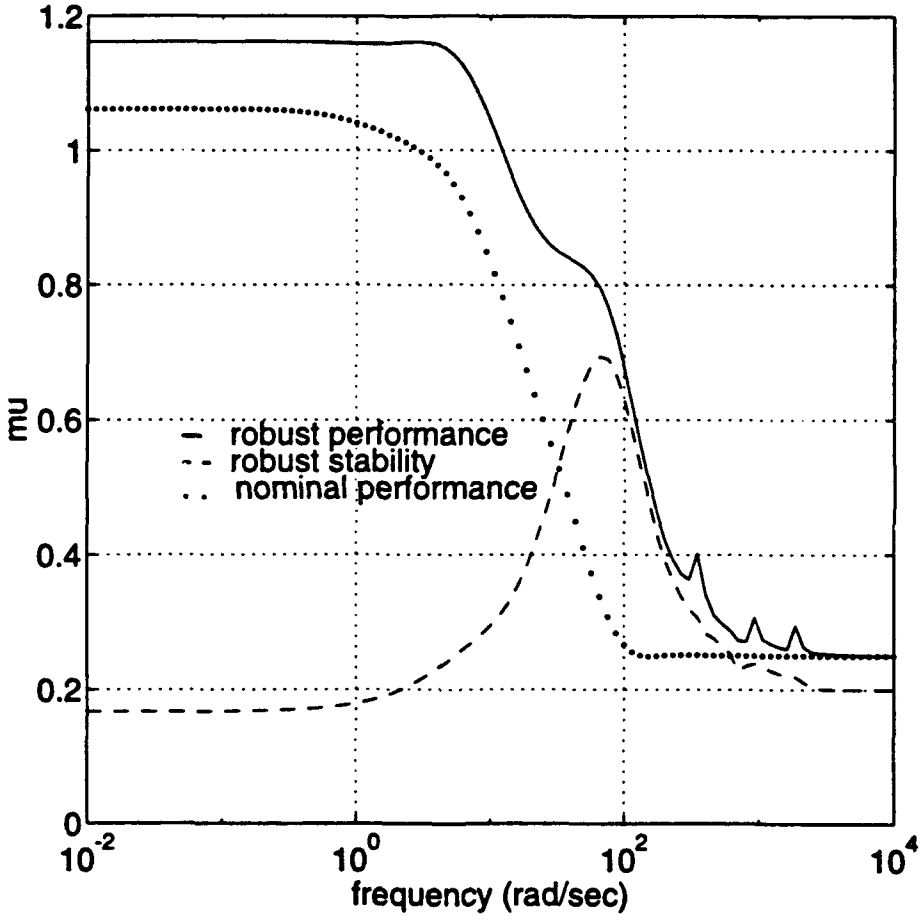

Figure 4.18: Robust analysis

TABLE 4.7: EIGENVALUE SENSITIVITY

			Eigenvalue Sensivitivy	
Eigenvalue	Parameter	Evaluated at	$\Delta\lambda/\Delta p$	$\mid \Delta\lambda/\Delta p \mid$
$-4.97 \pm j7.5$	M_α	M_{α_o}	$0 \pm j0.073$	0.073
		$M_{\alpha_o} + \Delta M_{\alpha_{max}}$	$0 \pm j0.038$	0.038
		$M_{\alpha_o} - \Delta M_{\alpha_{max}}$	$\pm 0.056 \pm j0$	0.056
	Z_α	Z_{α_o}	$0.5 \mp j0.02$	0.5
		$Z_{\alpha_o} + \Delta Z_{\alpha_{max}}$	$0.5 \mp j0.05$	0.5
		$Z_{\alpha_o} - \Delta Z_{\alpha_{max}}$	$0.5 \mp j0.01$	0.5
	M_q	M_{q_o}	$0.5 \pm j0.02$	0.5
		$M_{q_o} + \Delta M_{q_{max}}$	$0.5 \pm j0.03$	0.5
		$M_{q_o} - \Delta M_{q_{max}}$	$0.5 \pm j0.07$	0.5

a robust controller.

3. Uncertainty Reduction

The eigenvalues of the open loop system are

$$\lambda_{1,2} = -4.97 \pm j7.5$$

$$\lambda_{3,4} = -38.5 \pm j1923$$

$$\lambda_{5,6} = -7.36 \pm j368$$

$$\lambda_{7,8} = -18.7 \pm j937$$

$$\lambda_{9,10} = -132 \pm j135$$

Only $\lambda_{1,2}$ are affected by the variations in parameters M_α, Z_α and M_q. The eigenvalue sensitivities for these parameters is listed in Table 4.7. The parameters for scaling are selected by observing that the large variation in M_α causes the eigenvalues to vary from complex to real. While complex, the largest eigenvalue change is $\mid \Delta\lambda_{1,2} \mid = 7.5$, the distance from the nominal location to the real axis This change is already accomodated by the first 100% variation in M_α. On the real axis with all three parameters varying, the eigenvalues have extreme values of +5.10 and -15.1. The variation in M_α

alone causes the eigenvalues to move to +4.03 and -13.96. The additional eigenvalue change caused by variations in Z_α and M_q can be accommodated by increasing the variation in M_α to 300% and leaving unchanged the 15% variation in Z_α. An H_∞ controller is next designed for a system with these two uncertainties used in place of the uncertainty in M_q.

4. Controller Design for Reduced Uncertainties

Using only the scaled uncertainties in M_α and Z_α, a robust H_∞ controller was designed. The SSV plot for the closed loop system is shown in Figure 4.19. When tested against the system incorporating all three uncertainties at their actual values, the plot of Figure 4.20 results. The system meets the robustness specifications.

The time response of the final closed loop system was analyzed to assess performance. The step response of the system is show in Figure 4.21. The response shows an overdamped system with a rise time of approximately 0.15 seconds and no overshoot. The error at 1 second is 1.4%, and has decreased to near the 1% specification by 2 seconds.

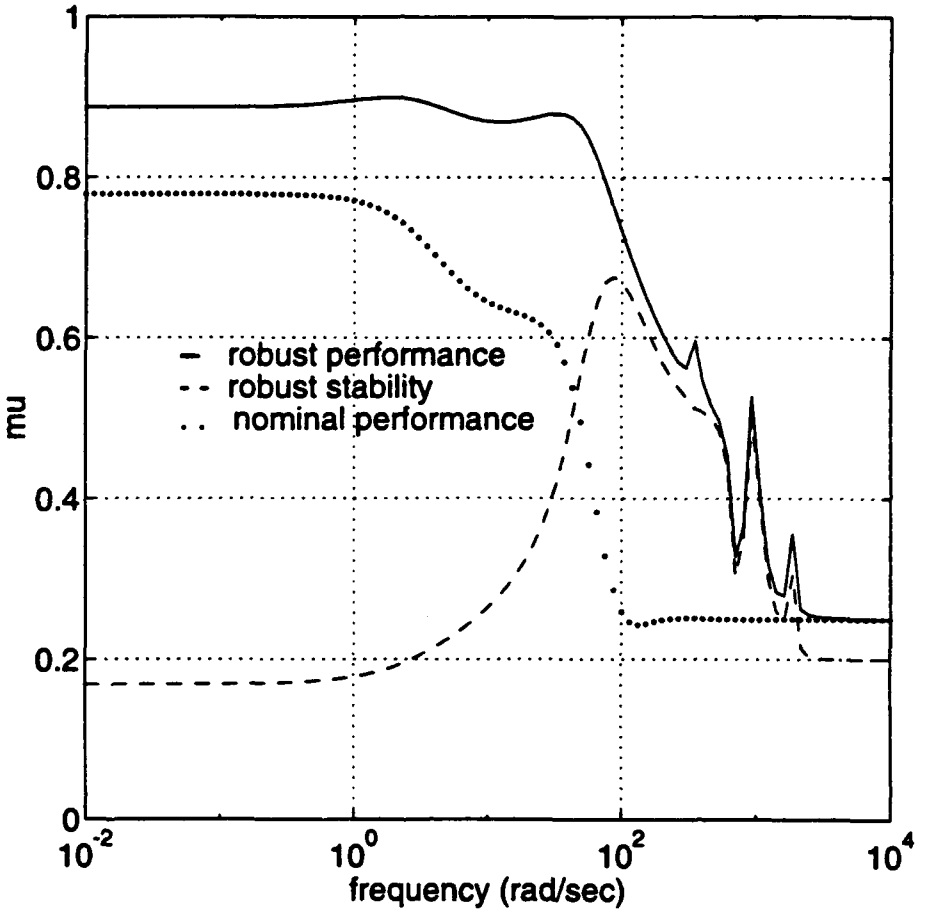

Figure 4.19: Robust analysis for scaled uncertainty plant

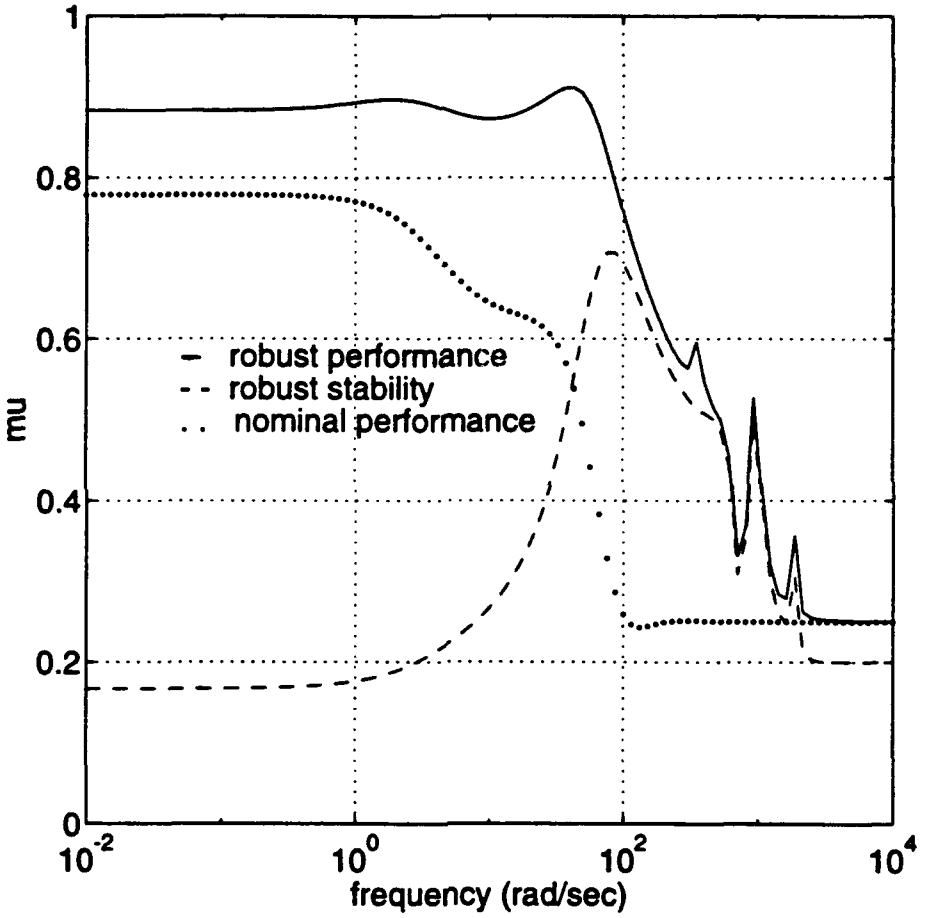

Figure 4.20: Robust analysis for plant with all uncertainties

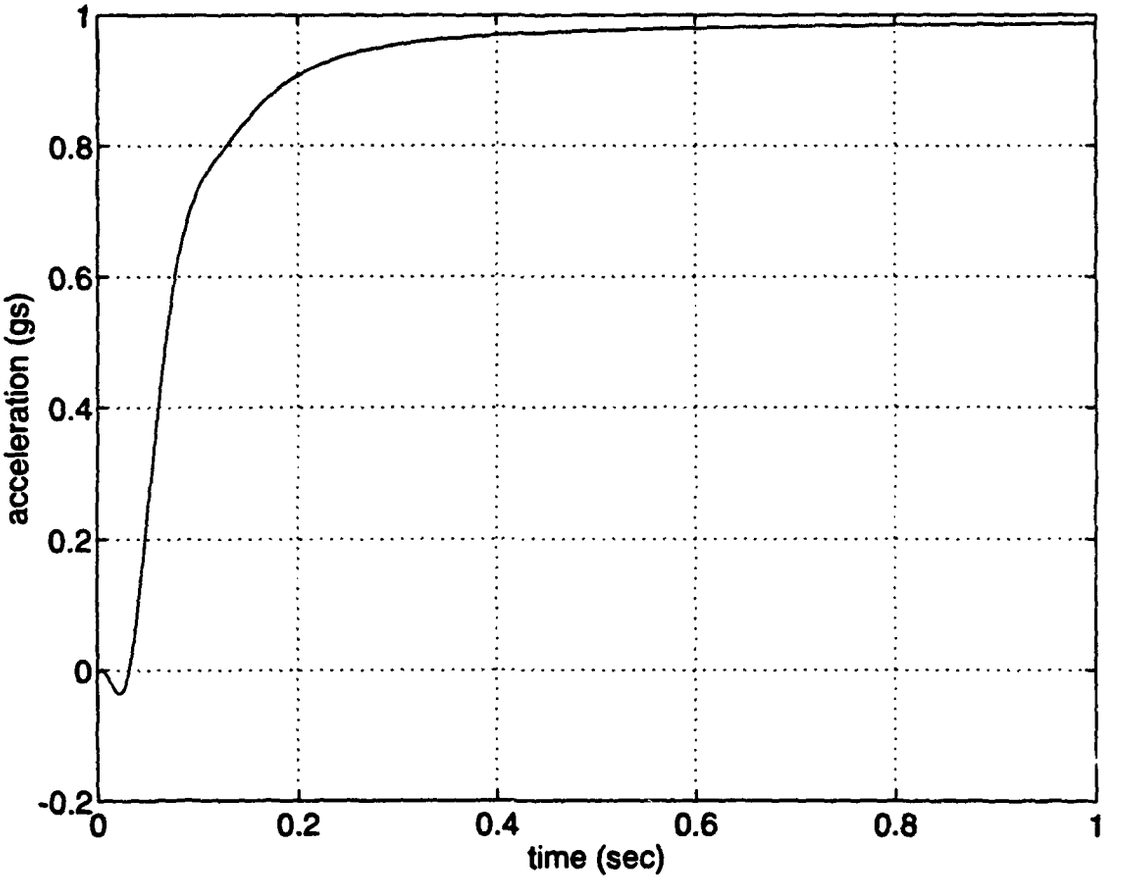

Figure 4.21: Step response

V. SUMMARY AND CONCLUSIONS

A. PROBLEM STATEMENT

Current H_∞ synthesis techniques are often unable to provide a robust controller design when all parametric uncertainties in a system are included in the plant model. The plant, in effect, becomes overconstrained and the design algorithms fail. This does not, however, preclude the existence of a robust H_∞ controller, rather it indicates current methods are not effective in many practical design problems. This work has focused on a technique which allows the designer to use existing H_∞ synthesis theory and commercially available software to produce a controller which is robust in the presence of all quantified parametric uncertainties in the plant. The procedure involves grouping uncertain parameters which affect the same open-loop eigenvalue. The variation of one or more of the designated parameters is scaled to provide for the same eigenvalue change as that caused by all the parameters at the extreme values of their uncertainties. An H_∞ controller which is robust in the presence of the scaled uncertainties is then shown to be robust in the presence of the actual plant uncertainties.

B. CONTRIBUTIONS

As a result of this research, two original contributions were made that pertain to robust controller design:

- Development of a technique which reduces the number of parametric uncertainties required for the design of a robust H_∞ controller that accommodates

all parametric uncertainties in the plant, when design attempts using all uncertainties have failed. This technique may also be used to reduce the number of uncertainties used even when a robust controller can be found for all uncertainties, thus reducing computation time.

- Procedures for applying the technique to missile autopilots, providing for the design of a robust controller taking into account not only model uncertainties but also parameter variations caused by changes in flight conditions. These variations, often quite extreme, have until now required conservative autopilot designs which sacrificed performance to maintain stability.

In short, this research has provided designers with a new tool for finding a robust H_∞ solution in specific cases when current design methods fail. Development of this technique has revealed several other areas requiring further study. These include:

- Complex scaling of a parametric variation rather than real scaling as described herein may allow for the use of a smaller scale factor in robust design, and therefore increase the number of problems for which a solution can be obtained.

- Performance functions in missile autopilot models are often the dominant constraints in controller design. A technique for reducing the number of performance constraints similar to the technique for parametric uncertainty reduction may also increase the number of problems for which a solution can be obtained.

APPENDIX A

Transfer Function Norms

Structured Singular Value (SSV) analysis makes extensive use of transfer function norms in defining the underlying theory for stability analysis. We present here a brief discussion of the 2-norm and ∞-norm along with some useful properties (Maciejowski, 1989).

Given a proper transfer function matrix $G(s)$ with no poles on the imaginary axis, the 2-norm of $G(s)$ is defined as

$$\|G\|_2 \equiv \sqrt{\frac{1}{2\pi}\int_{-\infty}^{\infty} tr[G(j\omega)G^T(-j\omega)]d\omega}.$$

The infinity norm is defined as

$$\|G\|_\infty \equiv \sup_\omega \bar{\sigma}(G(j\omega))$$

with $\bar{\sigma}$ denoting the largest singular value. These norms satisfy the following properties:

1. $\|G\| \geq 0$ with $\|G\| = 0$ if and only if $G = 0$.
2. $\|\alpha G\| = |\alpha|\|G\| \quad \forall\, \alpha \in \mathcal{C}$.
3. $\|G + H\| \leq \|G\| + \|H\|$.

The ∞-norm also satisfies

$$\|GH\|_\infty \leq \|G\|_\infty \|H\|_\infty.$$

This inequality is not satisfied by the 2-norm.

APPENDIX B

Robust Stability Analysis

We present in this Appendix a discussion of robust stability analysis using the small gain theorem (Burl, 1993). An uncertain system with a feedback controller designed for the nominal plant can be depicted as in Figure B.1. By combining the nominal plant and controller into one block $M(s)$, we can redraw the system as in Figure B.2. Writing the outputs of $M(s)$ in terms of the inputs:

$$\begin{bmatrix} y_d \\ y \end{bmatrix} = \begin{bmatrix} M_{11}(s) & M_{12}(s) \\ M_{21}(s) & M_{22}(s) \end{bmatrix} \begin{bmatrix} w_d \\ w \end{bmatrix}$$

Figure B.3 shows the system expanded to show the subsystems of $M(s)$. The nominal system $M(s)$ is stable since $K(s)$ is designed for the nominal plant. The entire system will therefore be internally stable provided that the loop containing $\Delta(s)$ is stable, since this is the only possible source of instability. The internal stability of this loop can be determined by examining the four transfer functions shown in Figure B.4. These can be written as

$$\begin{bmatrix} e_1 \\ e_2 \end{bmatrix} = \begin{bmatrix} (I - \Delta M_{11})^{-1} & (I - \Delta M_{11})^{-1}\Delta \\ (I - M_{11}\Delta)^{-1}M_{11} & (I - M_{11}\Delta)^{-1} \end{bmatrix} \begin{bmatrix} u_1 \\ u_2 \end{bmatrix}$$

Consider the transfer function from u_2 to e_1:

$$e_1 = (I - \Delta M_{11})^{-1}\Delta u_2$$

We can rewrite this as

$$e_1 = \Delta M_{11} e_1 + \Delta u_2.$$

Taking the 2-norm and employing some properties of norms from Appendix A:

$$\|e_1\|_2 = \|\Delta M_{11} e_1 + \Delta u_2\|_2 \leq \|\Delta M_{11} e_1\|_2 + \|\Delta u_2\|_2$$

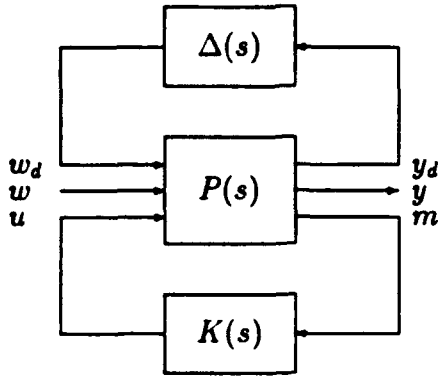

Figure B.1: Uncertain system with feedback control

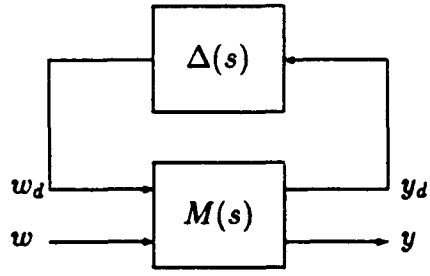

Figure B.2: Uncertain system in standard form

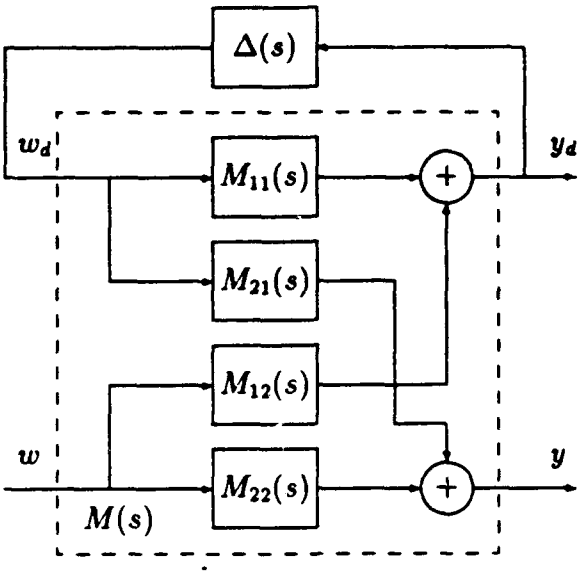

Figure B.3: System expanded to show subsystems of $M(s)$

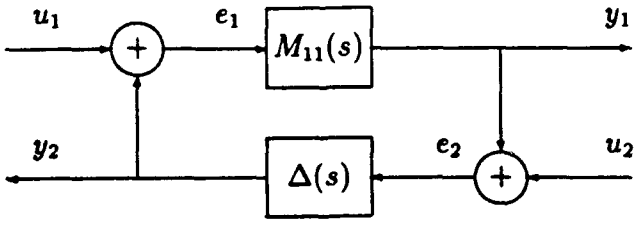

Figure B.4: System used for stability analysis

$$\|e_1\|_2 \leq \|\Delta M_{11}\|_\infty \|e_1\|_2 + \|\Delta\|_\infty \|u_2\|_2$$

$$\|e_1\|_2 \leq \|\Delta\|_\infty \|M_{11}\|_\infty \|e_1\|_2 + \|\Delta\|_\infty \|u_2\|_2$$

We can solve for the 2-norm of e_1:

$$\|e_1\|_2 \leq (1 - \|\Delta\|_\infty \|M_{11}\|_\infty)^{-1} \|u_2\|_2 \tag{B.1}$$

Noting that $\|\Delta\|_\infty \leq 1$, this inverse is finite if

$$\|M_{11}\|_\infty < 1.$$

Analysis on the other transfer functions yields the same conclusion. We can now state that for the uncertain system of Figure B.2 where the perturbation matrix is bounded such that

$$\|\Delta\|_\infty \leq 1,$$

internal stability is guaranteed for all allowable perturbations provided that $M(s)$ is nominally stable and

$$\|M_{11}\|_\infty < 1.$$

APPENDIX C

Guaranteed Gain and Phase Margins Using the Sensitivity Function

In this appendix we derive one method for providing guaranteed gain and phase margins for a mulit-input multi-output system by using a scalar input feedback uncertainty (Dailey, 1990). Consider the plant in Figure C.1. The uncertainty blocks are arranged in a feedback loop. When the perturbations Δ_i are combined into a single diagonal block as shown in Figure C.2, the transfer function seen by $\mathbf{\Delta}$ is $(I - KG)^{-1}$. We recognize this as S, the sensitivity function. An equivalent system is shown in Figure C.3. In this diagram, $\mathbf{\Delta} = I - C^{-1}$, $L = KG$ is the loop gain and C is a diagonal matrix. The gain seen by L is equal to $(I - (I - C^{-1}))^{-1} = C$. Thus, the elements of C are simply gains for each path in the loop. From the results of the stability analysis in Appendix B, a guaranteed upper bound on the gain of $\mathbf{\Delta}$, namely $\bar{\sigma}(\mathbf{\Delta})$, for the feedback loop to remain stable can be determined from

$$\bar{\sigma}(\mathbf{\Delta})\bar{\sigma}(S) < 1 \quad \forall \ \omega \tag{C.1}$$

Since the maximum singular value is independent of the phase of the matrix elements, each diagonal element Δ_i in $\mathbf{\Delta}$can be expressed as a magnitude and phase, $\mid \Delta_i \mid e^{j\theta}$, $\theta \in [0, 2\pi]$. From Equation C.1, $\bar{\sigma}(\mathbf{\Delta}) \leq 1/\bar{\sigma}(S)$ is required for stability. Now, solving for the gain matrix C from above yields $C = (I - \mathbf{\Delta})^{-1}$. This matrix has elements $1/(1 - \Delta_i)$ on the diagonal. Assuming only real perturbations, the gains will vary from $1/(1- \mid \Delta_{i_{max}} \mid)$ to $1/(1+ \mid \Delta_{i_{max}} \mid)$. Observing that for a diagonal matrix, $\mathbf{\Delta}$, $\bar{\sigma}(\mathbf{\Delta}) = \mid \Delta_{i_{max}} \mid$, the stability requirement yields

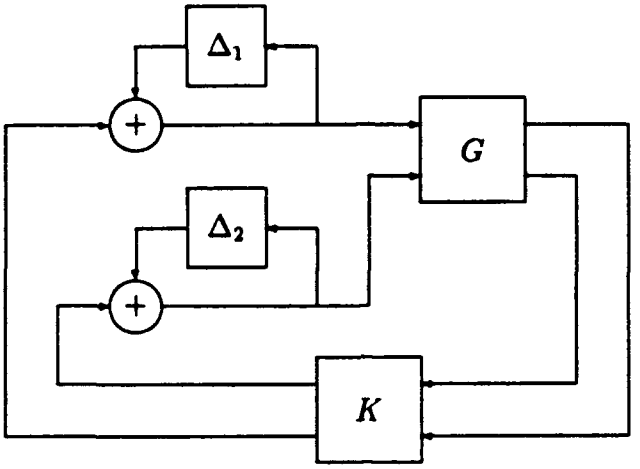

Figure C.1: Closed loop plant with input feedback

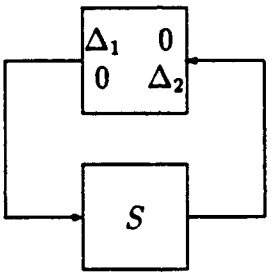

Figure C.2: Closed loop plant with diagonal feedback block

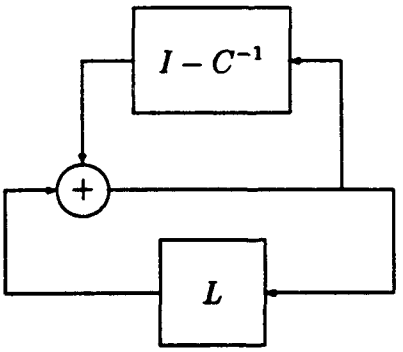

Figure C.3: Loop gain

$$| \Delta_{i_{max}} | = \inf_{\omega \in R} \frac{1}{\bar{\sigma}(S)} \tag{C.2}$$

Thus, the gain margins are given by $[\frac{1}{1-|\Delta_{i_{max}}|} \ \frac{1}{1+|\Delta_{i_{max}}|}]$. Figure C.4 shows a plot of $| \Delta_{i_{max}} |$ versus gain margin in dB. It can also be shown that the guaranteed lower bound for the multi-input multi-output phase margin is given by

$$\text{PM} \in [-\theta, +\theta] \ \text{ where } \theta = 2sin^{-1}(\frac{| \Delta_{i_{max}} |}{2})$$

Figure C.5 shows a plot of $| \Delta_{i_{max}} |$ versus phase margin in degrees.

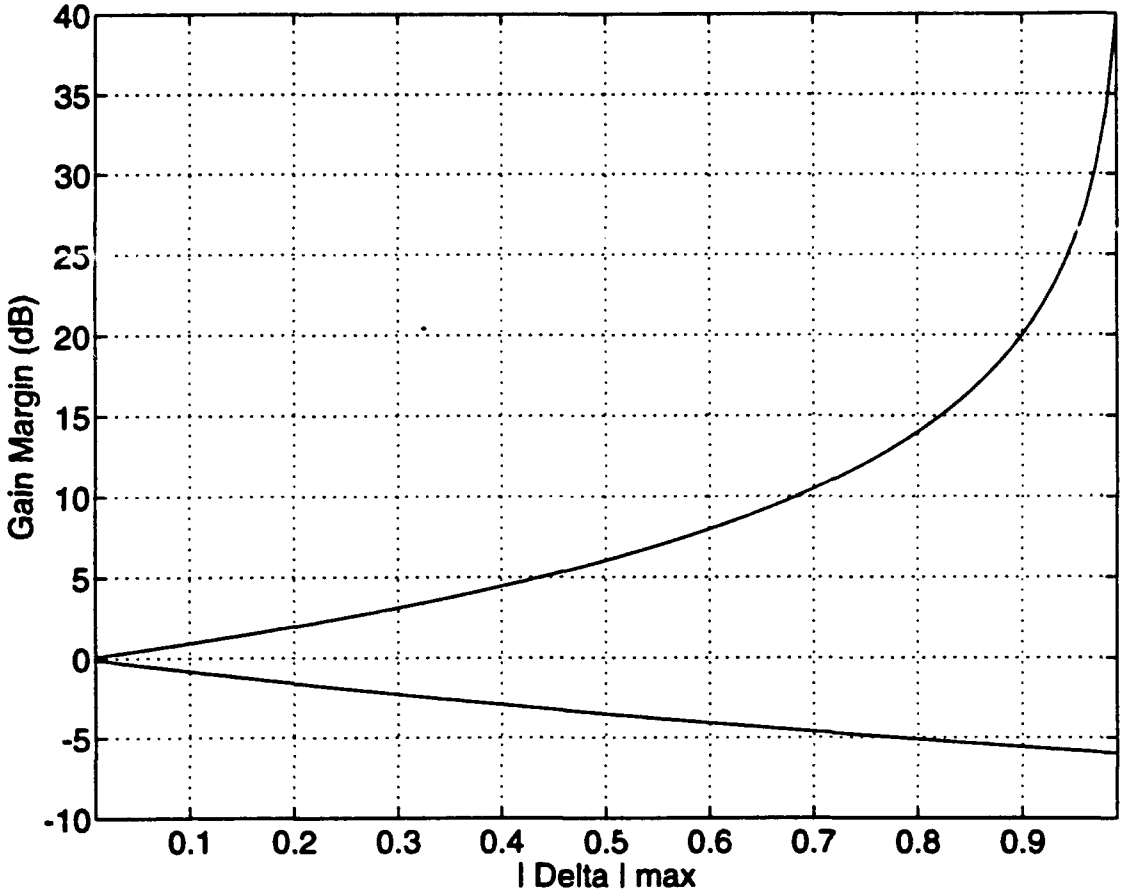

Figure C.4: Gain margin in dB versus $| \Delta_{i_{max}} |$

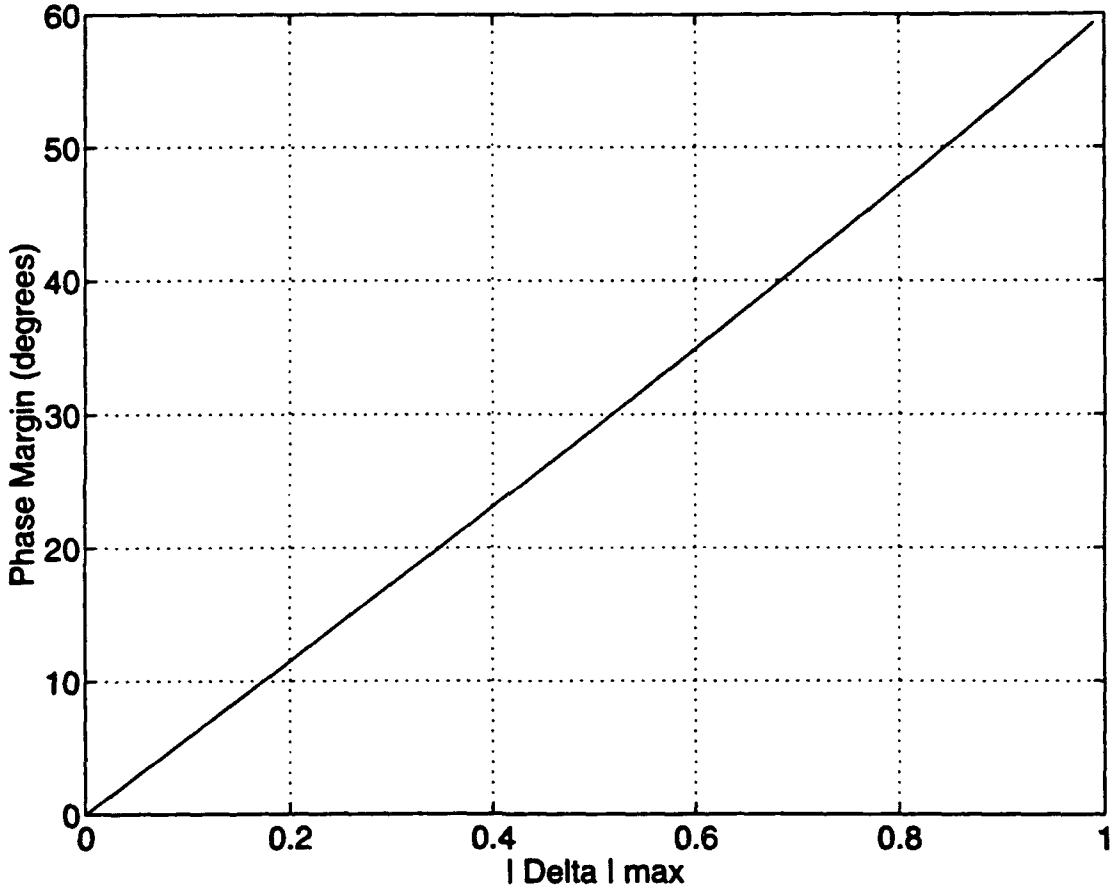

Figure C.5: Phase margin in degrees versus $| \Delta_{i_{max}} |$

LIST OF REFERENCES

Balas, G. J., Doyle, J. C., Glover, K., Packard, A., Smith, R., *μ-Analysis and Synthesis Toolbox User's Guide*, MuSyn, Inc., Minneapolis, MN, 1991, pp. 3-4/7.

Belcastro, C. M. and Chang, B.-C., "On Parametric Uncertainty Modeling for Real Parameter Variations," *Proceedings of the 31st Conference on Decision and Control*, IEEE, Vol. 1, December 1992, pp 674-679.

Bibel, J.E. and Malyevac, D. S., "Guidelines for the Selection of Weighting Functions for H-Infinity Control," Technical Note NSWCDD/MP-92/43, Naval Surface Warfare Center, Dahlgren Division, Dahlgren, VA, January 1992.

Bibel, J.E. and Stalford, H.L., "An Improved Gain-Stabilized Mu-Controller For A Flexible Missile," *AIAA 30th Aerospace Sciences Meeting & Exhibit*, AIAA-92-0206, January 1992.

Burl, Jeffery B., "Linear Optimal Estimation and Control," (Unpublished manuscript).

Chen, B.M., Saberi, A. and Ly, Uy-Loi, "Exact Computation of the Infimum in H_∞ -Optimization Via Output Feedback," *IEEE Transactions on Automatic Control*. Vol. 37, No. 1, January 1992, pp. 70-78.

Dailey, R.L., "Lecture Notes for the Workshop on H_∞ and μ Methods for Robust Control," American Control Conference, San Diego, CA, 1990.

de Gaston, R.R.E. and Safonov, M.G., "Exact Calculation of the Multiloop Stability Margin," *IEEE Transactions on Automatic Control*, Vol. 33, No. 2, February 1988, pp. 156-171.

Doyle, J.C., "Guaranteed Margins for LQG Regulators," *IEEE Transactions on Automatic Control*, Vol. AC-23, 1978, pp. 756-757.

Doyle, J.C., "Analysis of Feedback Systems With Structured Uncertainties," *IEEE Proceedings*, Vol. 129, Pt. D., No. 6, November 1982, pp. 242-250.

Doyle, J.C., Glover, K., Kharogonekar, P.P. and Francis, B.A., "State-Space Solutions to Standard H_2 and H_∞ Control Problems," *IEEE Transactions on Automatic Control*, Vol. 34, No. 8, August 1989, pp. 831-846.

Elgersma, M., Freudenberg, J. and Morton, B., "Polynomial Methods for the Structured Singular Value with Real Parameters," *Proceedings of the 31st Conference on Decision and Control*, IEEE, Vol. 1, December 1992, pp. 237-242.

Francis, B.A., "A Course in H_∞ Control Theory," *Lecture Notes in Control and Information Sciences*, Springer-Verlag, New York, 1987.

Safonov, M. G., "Stability margins of diagonally perturbed multivariable feedback systems," *IEEE Proceedings*, Pt. D., November, 1982, pp. 251-256.

Zames, G., "Feedback and Optimal Sensitivity Model Reference Transformations, Multiplicative Seminorms and Approximate Inverses," *IEEE Transactions on Automatic Control*, 1981, pp. 585-601.

INITIAL DISTRIBUTION LIST

1.	Defense Technical Information Center Cameron Station Alexandria, VA 22304–6145	2
2.	Dudley Knox Library Code 52 Naval Postgraduate School Monterey, CA 93943–5101	2
3.	Chairman, Code EC Department of Electrical and Computer Engineering Naval Postgraduate School Monterey, CA 93943–5121	2
4.	Prof. Roberto Cristi, Code EC/Cx Department of Electrical and Computer Engineering Naval Postgraduate School Monterey, CA 93943–5121	2
5.	Prof. Harold Titus, Code EC/Ts Department of Electrical and Computer Engineering Naval Postgraduate School Monterey, CA 93943–5121	1
6.	Prof. James H. Miller, Code EC/Mr Department of Electrical and Computer Engineering Naval Postgraduate School Monterey, CA 93943–5121	1
7.	Prof. Daniel Collins, Code AA/Co Department of Aeronautical and Astronautical Engineering Naval Postgraduate School Monterey, CA 93943	1
8.	Prof. Anthony Healey, Code ME/Hy Department of Mechanical Engineering Naval Postgraduate School Monterey, CA 93943	1

9.	Prof. Jeffery B. Burl Michigan Technological University 1400 Townsend Drive Houghton, MI 49931-1295	1
10.	Director, Strategic Systems Programs Attn: Mr. Marcus Messerole Washington, DC 20376	1
11.	Commander, Naval Surface Warfare Center Attn: Mr. John Bibel Dahlgren, VA 22448	1
12.	Commander, Naval Air Warfare Center Attn: Mr. Allen Robins China Lake, CA 9355-6001	1
13.	Commanding Officer, Strategic Weapons Facility, Pacific Attn: Lieutenant Commander David L. Krueger (SPB 30) 6401 Skipjack Circle Silverdale, WA 98315-6499	2